Addis Ababa University
Addis Ababa Institute of Technology
School of Electrical and Computer Engineering

Particle Swarm Optimization Tuned Sliding Mode Control of Switched Reluctance Motor for EV Application

A thesis submitted to School of Graduate Studies, Addis Ababa Institute of Technology, Addis Ababa University in partial fulfillment of the requirement for the Degree of Master of Science in Electrical Engineering (Control Engineering)

By

Aschalew Nigussie

Advisor

Dr.Mengesha Mamo(PHD)

January 21, 2022

Addis Ababa, Ethiopia

Addis Ababa University

Addis Ababa Institute of Technology

School of Electrical and Computer Engineering

Particle Swarm Optimization Tuned Sliding Mode Control of Switched Reluctance Motor for EV Application

By: Aschalew Nigussie

APPROVED BY BOARD OF EXAMINERS

Name	Signature	Date
Dr.Bisrat Derebssa (School Dean)	.....	.....
Dr.Mengesha Mamo (Advisor)	.....	.....
Dr.Dereje Shiferaw (Internal Examiner)	.....	.....
Mr.Yalemzerf Getnet (External Examiner)	.....	.....

Declaration

I declare that the work entitled "PSO Tuned Sliding Mode Control of SRM for EV Application" is my original work and has not been presented for any degree in any university or college, and sources of material used for the thesis is well acknowledged.

Name	Signature	Date
Aschalew Nigussie	.....	.....

Acknowledgment

I would like to express my special thanks of gratitude and appreciation to my advisor **Dr.Mengesha Mamo** who has given me wonderful support and for the valuable information that he shared with me throughout the whole work. I have learned valuable lessons from his perception, wariness, and ideas.
In addition to **Dr.Mengesha Mamo**, I would like to extend my thanks of gratitude to **Dr.Dereje Shiferaw** and **Dr.Lebsewerk Negash** for their time dedicated to supervising and reviewing my work and also for their valuable suggestions.
Lastly, I would like to thank my family and friends who helped me a lot to finalize this thesis. Without that support, I could not have finished this thesis.

Aschalew Nigussie

Abstract

In this thesis, a sliding mode speed controller along with the particle swarm optimization algorithm and discrete commutation logic of switched reluctance motor is presented. The switched reluctance motor has several interesting advantages. For instance, the switched reluctance motor has high starting torque, a wide speed range, heat-tolerant capability, and a simple braking mechanism, which make it attractive for electric vehicles (EVs) traction applications. The switched reluctance motor has high torque ripples which affect the performance of the motor, and it is a highly nonlinear plant due to the doubly salient structure.

A performance comparison of conventional proportional integral speed controller with sliding mode speed controller is presented for the 10/8 Switched Reluctance Motors. A robust controller is advised for high-performance control of switched reluctance motors. The effectiveness of the sliding mode controller for the SRM is confirmed by simulation results. The proposed controller guarantees that the actual motor speed tracks the reference speed slightly faster than the proportional-integral controller. The speed difference between the actual and the reference for a PI speed controller is 0.18% while for the SMC is 0.0002% which implies the PI has larger steady state error. The robustness of the proposed controller to sudden disturbances is also validated through simulation studies. The sliding mode speed controller parameters are obtained with the help of the Particle Swarm Optimization (PSO) algorithm while the PI speed controller gains are obtained using trial and error.

The performance of the loaded Switched Reluctance Motor (SRM) is tested and evaluated with the help of simulation. The vehicle is modeled in MATLAB/SIMULINK and developing the torque-speed characteristics that represent the vehicle load type. The SRM reached its steady-state velocity of $570.74RPM$ in $13sec$ and also it took $4.5sec$ to stop the vehicle from running at a steady-state speed.

Key Words : Switched Reluctance Motor, Electric vehicle, PSO, Sliding Mode Controller.

Contents

List of Figures

List of Tables

List of Abbreviations

$T-OFF$	Turn OFF angle
$T-ON$	Turn ON angle
AC	Alternating Current
BJT	Bipolar Junction Transistor
D.R	Duty Ratio
DC	Direct Current
emf	Electromotive Force
EV	Electric Vehicle
HEV	Hybrid Electric Vehicle
KVL	Kirchhoff's Voltage Law
MOSFET	Metal-Oxide-Semiconductor Field-Effect Transistor
PI	Proportional Integral
PM	Permanent Magnet
PSO	Particle Swarm Optimization
PWM	Pulse Width Modulation
SMC	Sliding Mode Control
SRM	Switched Reluctance Motor

Chapter 1

Introduction

1.1 Background of Study

Electric vehicles (EVs) are automobiles that use the electric machine for their traction. Electric vehicles are becoming increasingly important not only do they reducing noise and pollution, but also they can be used to reduce the dependence of transport on oil and to reduce carbon emissions [1]. Electric vehicles are normally accompanying with benefits to the environment and saving energy. These benefits comprise reducing local pollution from the vehicles themselves, reducing dependency on oil and other fossil fuels, and reduction of carbon emissions to the atmosphere. The electric vehicle consists of a power supply unit for energizing the motor, an electric motor for traction of the vehicle, and a controller. The controller will normally control the power supplied to the motor, and hence the vehicle speed, in forward and reverse direction.

The most widely used electric motor for EV traction application is the permanent magnet synchronous motors (PMSMs), and an induction motor. This is because of the reality that a permanent magnet and an induction motor have a quality to achieve high torque densities, wide speed range, and high starting torque which makes those machines attractive for EV traction. On the other hand, the inclusion of a magnet in permanent magnets and is very costly and the heat contributing winding in an induction motor limits somehow the effectiveness of those motors for EV traction application [2].

Electric machines without rare earth materials show an expanding interest to reach and accomplish comparable performance of the other machines. Among the distinguishing existing magnet-free machines, there is much interest in the switched reluctance motors for the propulsion of electric vehicles due to simple mechanical

construction and simple design with the capability to operate in a hazard-free environment at very high speed [3], [4].

In recent years, an exceptional interest in using switched reluctance machines due to their several advantages over other electrical machines. The rotor of switched reluctance motor (SRM) has no winding, which gives more preference to the machine, including smaller size, lowest costs, higher speeds, high power density, high starting torque, wide speed range, and fault-tolerant capability [5]. Double saliency structure, inherent magnetic saturation, and time variation of parameters induce nonlinear complexity, high uncertainties in the dynamics, and torque ripple in the SRM [6].

The switched reluctance motor has a highly non-linear dynamic system due to its double saliency. In this thesis, a simple non-linear controller named sliding mode control is used to adapt the motor for EV application and an optimization algorithm is incorporated to tune the controller gains that replace the complex mathematical analysis. The torque ripple minimization is done by adjusting the commutation system.

1.2 Statement of The Problem

For the time being, one major concern of the world is about the environment which is affected by many factors. One such factor is the internal combustion engine vehicles which emit carbon dioxide to the environment. The internal combustion engine vehicles also require high maintenance. Thus, by considering the above factors in mind it is essentially replacing the internal combustion engine vehicles with an electric vehicle. However, the replacement of ICE with an electric motor should consider parameters like; the speed of the vehicle, weight, cost, comfort, reliability, and compactness.

In recent years electric vehicles are popular, but they use an induction motor, PMSM, and DC as a propulsion section. In this thesis switched reluctance motor is used for electric vehicle traction application which overcomes the deficiencies in other electrical motors. The benefits gained from the SRM are; wider speed range, higher power density, low cost, fault-tolerant, high starting torque, a simple braking system, and cheaper power converter circuit. The SRM is a highly non-linear system and it has high torque ripple due to a double sailency. The torque ripple affects the overall performance of the drive system. Thus, it is required a simple non-linear controller to control the SRM drive used for variable speed drive application and further to reduce the torque ripples. Such a controller is a sliding mode control tuned with a particle swarm optimization algorithm along with the commutation.

1.3 Objectives of The Study

1.3.1 General Objective

The main objective of this thesis is to design the sliding mode control for switched reluctance motor and tuning using a particle swarm optimization algorithm to adapt for EV drive application.

1.3.2 Specific Objectives

- To design a sliding mode speed controller for switched reluctance motor.
- To tune sliding mode controller parameters using the PSO algorithm.
- To model and simulate a 200 kg vehicle on a flat ground in MATLAB®/SIMULINK® .

1.4 Significance of the Research

One of the main challenges in the control of the switched reluctance motors is designing a stable controller taking into account the system nonlinearity. The design of stable and robust nonlinear controllers is one of the significant problems on which scholars have been focused. The sliding mode control is verified to have a capability to preserve the control stability in various systems that exposes to the disturbances and parameter variations in the system.

In recent years, different classes of the control method have been found in the literature, in the implementation toward the difficulties in the control of switched reluctance motor. The raised numbers of works conducted with the control of the switched reluctance motor have been proposed extended from linear control to nonlinear control strategies. One of the simple nonlinear control structure is the sliding mode controller, which is suitable for regulating the SRM drive to find the application in EV traction.

1.5 Thesis Organization

The thesis is organized into six chapters including this introduction. The rest of the thesis is organized as follows.

Chapter 2 Introduce general definition and electrical circuit of a typical switched reluctance motor and also describe the basic principle of its operation. In addition, the converter circuit, PSO, theory of the sliding mode controller and related works are presented in this chapter.

Chapter 3 Deals with the design of discrete commutation system and the design of the proposed controller along with the optimization method.

Chapter 4 describes vehicle design and its characteristics.

Chapter 5 Presents the simulation results obtained and analysis on those results.

Chapter 6 concludes the whole thesis adding recommendation and future works to be done.

Chapter 2

Literature survey

2.1 Introduction

In this chapter, principles of operation, torque generation, the theoretical background about the distinguishing features of SRM to other conventional machines along the converter used to supply the designated motor are discussed. In addition, the theory of the proposed controller, particle swarm optimization, and related works are also involved in this chapter.

2.2 Switched reluctance motor

The switched reluctance motor is a type of electromagnetic rotary machine during which, the torque is produced due to the tendency of its movable part to move to a position where the inductance of the energized phase winding is maximized (or a position to a minimum reluctance). Switched reluctance motor manufacturers privilege better performance and reliability, higher efficiency, and lower cost than conventional induction or other variable speed motors. In SRM both the torque produced and the inductance depend on the stator current i_s and rotor position θ, this makes the designated motor highly nonlinear and difficult to control. The switched reluctance motor is gaining much attention in industrial applications such as wind energy systems and electric vehicles due to its rugged and simple construction, wide-speed range operation capability, insensitivity to high temperature, and fault tolerance [7],[3].

2.2.1 Switched Reluctance Motor Construction

The switched reluctance motor is simple and rugged. It is a doubly salient type of motor. A Five-phase switched reluctance motor has 10 poles on the stator side and

8 poles on the rotor side. However, the rotor has no windings or Permanent magnet it only consists of steel. The stator poles consist of a concentrated winding around them and each pair of diametrically located opposite coils form one phase of the motor. The construction feature of a typical 10/8 poles switched reluctance motor is shown in the figure below.

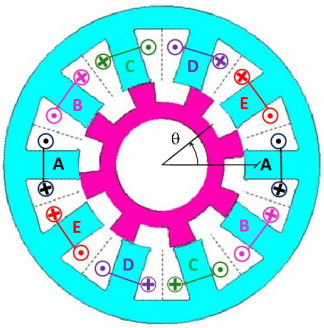

Figure (2.1) Cross-section of Five phase 10/8 pole SRM [8]

2.2.2 Operation Principles of Switched Reluctance Motor

The working principle of the switched reluctance motor is pretty simple. let us taking an iron piece, If we keep that in a magnetic field, the iron piece will be aligned to the minimum reluctance position and get locked magnetically [9]. A similar principle is followed in a switched reluctance motor. As the name indicates, a switching power converter is needed for the operation of the switched reluctance motor. It works on the principle of variable reluctance, meaning, the rotor always tries to align along with the minimal reluctance pathway. The minimum reluctance(or maximum inductance) portion of the rotor attempts to align itself with the stator magnetic field. Hence, the reluctance torque is established in the rotor. This motor utilizes the fact that the forces from a magnetic field on the iron in the rotor can be up to ten times bigger than the magnetic forces on the current-carrying conductors [10].

A switched reluctance motor operates by exciting the stator windings in response to a change in the magnetic circuit formed by the rotor and stator parts. The stator of a switched reluctance motor contains windings, similar to other electric motors, but the rotor is simply made of steel that is shaped into salient poles, with no windings or magnets either [11].

2.2.3 Equivalent Circuit of Switched Reluctance Motor

Like other electrical machines switched reluctance motor is also represented as an R-L circuit as shown in the figure 2.2 [10].

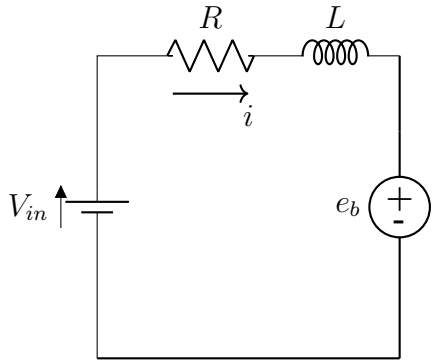

Figure (2.2) Single phase equivalent circuit of SRM

The voltage across the terminals of a single phase of an SRM winding is associated to the flux linked in the winding by Faraday's law as,

$$V = i * R_s + \frac{\mathrm{d}\psi(\theta, i)}{\mathrm{d}t} \tag{2.1}$$

Where R_s is per phase resistance,ψ is per phase flux linked by the winding and i is the motor current.

As a consequence of the double salient construction of the SRM (both the rotor and the stator have salient poles) and because of magnetic saturation effects, as a whole, the flux linked in an SRM phase winding varies as a function of rotor position,θ, and the motor current i.

Thus, the second term on the right side of equation (2.1) can be expressed as;

$$\frac{\mathrm{d}\psi(\theta, i)}{\mathrm{d}t} = \frac{\partial\psi}{\partial i} * \frac{\mathrm{d}i}{\mathrm{d}t} + \frac{\partial\psi}{\partial\theta} * \frac{\mathrm{d}\theta}{\mathrm{d}t} \tag{2.2}$$

Substituting the expression in equation (2.2) in to equation (2.1) becomes;

$$V = Rs * i + \frac{\partial\psi}{\partial i} * \frac{\mathrm{d}i}{\mathrm{d}t} + \frac{\partial\psi}{\partial\theta} * \frac{\mathrm{d}\theta}{\mathrm{d}t} \tag{2.3}$$

Where $\partial\psi/\partial i$ is the incremental inductance, $\partial\psi/\partial\theta$ is the back EMF coefficient, and $\mathrm{d}\theta/\mathrm{d}t$ is the speed ω.

2.3 Principles of Torque Generation in SRM

Equation (2.3) governs the transfer of electrical energy into the SRM's magnetic field. In this section, the equations which describe the conversion of the field's

energy into mechanical energy is developed.
Multiplying each side of (2.1) by the electrical current, i, gives an expression for the instantaneous input power of an SRM,

$$p_i = i^2 * R_s + i * \frac{\mathrm{d}\psi(\theta, i)}{\mathrm{d}t} \tag{2.4}$$

Where p_i is the input power to the motor, $i^2 R_s$ is the copper loss in the winding and $i * {}^{\mathrm{d}\psi(\theta,i)}/_{\mathrm{d}t}$ represents the sum of output powers stored in the field and the mechanical power.
Thus,

$$i * \frac{\mathrm{d}\psi(\theta, i)}{\mathrm{d}t} = \frac{\mathrm{dW_f}}{\mathrm{d}t} + \frac{\mathrm{dW_m}}{\mathrm{d}t} \tag{2.5}$$

Where ${}^{\mathrm{dW_f}}/_{\mathrm{d}t}$ is the power stored in the field and ${}^{\mathrm{dW_m}}/_{\mathrm{d}t}$ represents the instantaneous mechanical power. Inserting the expression for co-energy in to the torque equation gives as;

$$T = \frac{\mathrm{d}W_c}{d\theta}, but W_c = \frac{i^2}{2} L(\theta) \tag{2.6}$$

Then the simplified expression for the developed torque by the motor is as follows.see A

$$T = \frac{i^2}{2} * \frac{\mathrm{d}L}{d\theta} \tag{2.7}$$

From the simplified torque equation, it is clear that the direction of torque developed by the motor depends on the gradient of inductance with respect to rotor position. This torque expression of the SRM makes the braking techniques easier than other conventional AC or DC machines.

2.4 Power Converters

Power converter is the one components of derive system and its function is to deliver appropriate power to the motor from battery or DC source. The motor torque in switched reluctance motors is proportional to the square of the current so that the converter has to supply the motor with a unidirectional current. Hence, converters feeding the SRM are of the unipolar type and they generally use two switch per phase[12].
The value of actual conduction angles α_z is always higher than the stroke angle s as a result of current rise and decline in the phase winding and, hence, in the operation of the SRM motor, there are periods when 2 or even 3 phase windings are in conducting ('ON') state. Since the goal is to gain high values of average electromagnetic torque, the period of conduction is extended in the range of strong attraction of the rotor tooth by the electromagnet made up in a pair of stator teeth. Therefore, the

switch off-angle only slightly goes before the aligned position. Consequently, the process of current decay within a given phase is faster as much as possible to avoid negative torque (generating torque) values. This happens after the rotor reaches the position determined by the angle $T - OFF$, as a result of energizing this winding with the reverse voltage $-V_s$ which supplies the phase and, thus, causing the energy to return to the source. Such capability has to be held through the commutation system of the phases of the SRM motor.

The basic system of the power supply and commutation of a single-phase winding of SRM involves an asymmetric transistor/diode H bridge shown in Figure 2.3. Since SRM is a reluctance motor type and the direction of the torque is not depending on the direction of the current flow through the phase winding, so, the converter does not need to facilitate the current flow through the phase winding in both directions and it is enough to apply two power transistors and two diodes to guarantee energy supply and energy return back to the source. Over the period when winding is in supply state from the source both the transistors S_1 and S_2 are in the ON state which is called hard switching mode.

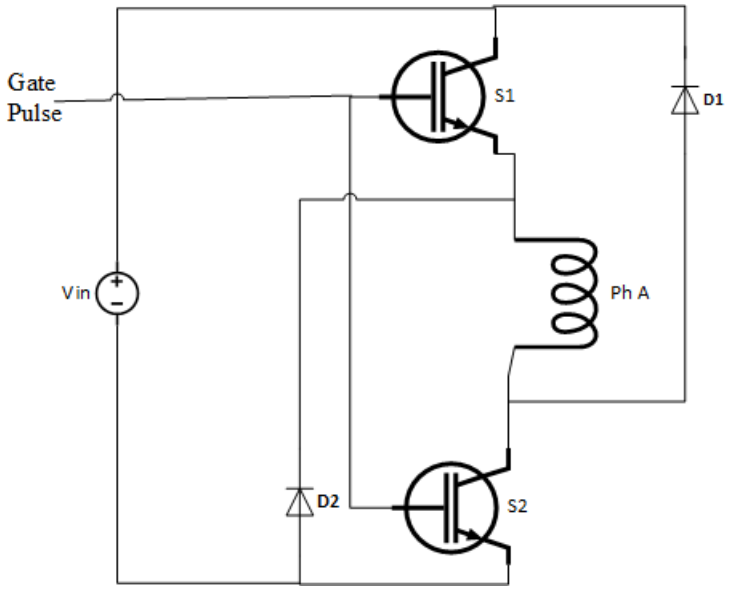

Figure (2.3) Converter Topology for a single phase

2.5 Particle Swarm Optimization

Particle swarm optimization is a method that optimizes a problem by iteratively trying to improve a problem solution about a given measure of value. It solves a given problem by having a population of candidate solutions, named particles, and moving these particles around in the search-space (possible solution areas) according to simple mathematical formula over the particle's position and its velocity.

The particle's movement is manipulated by its local best-known position but is also directed towards the best-known positions in the entire search space, which are updated as better positions are found by other particles. This is expected to move the population toward the best solutions[13].

Particle swarm optimization (PSO) is a type of the evolutionary computations methods. Similar to the other evolutionary computation methods, PSO is a population-based search algorithm and it is initialized with a population of a random solution, so-called particles. Unlike in the other evolutionary computation methods, each particle in a PSO is also associated with the velocity of each particle [14]. Particles fly through the search space with velocities that are dynamically attuned according to their historical behaviors. Thus, the particles tend to fly towards the best search area over the entire course of the search process [15].

The PSO algorithm is discovered through a simplified social model. It is related to bird flocking, fish schooling, and swarm (population) theory. The PSO was first designed to simulate birds looking for food which is defined as a "cornfield vector." The bird would find food through social cooperation with other neighborhood birds around it. It was then extended to a multidimensional search [16]. The PSO algorithm is described as below;

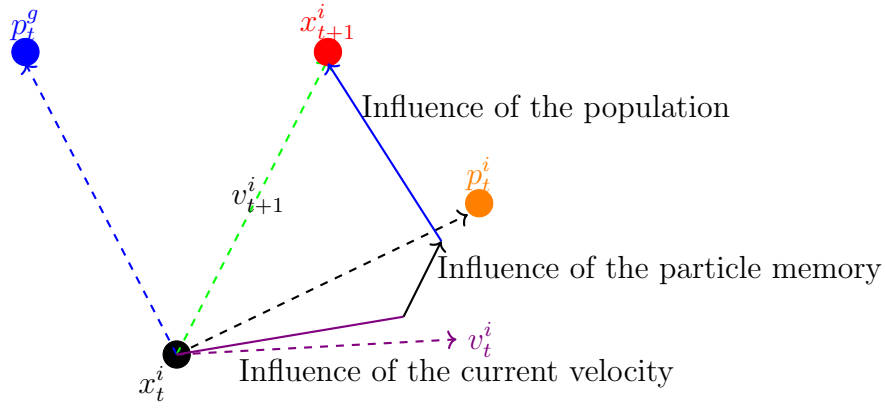

Figure (2.4) Particle's Iteration Scheme

$$V_{id} = c_1 rand()(p_{id} - x_{id}) + c_2 Rand()(p_{gd} - x_{id}) \tag{2.8}$$

$$x_{id} = v_{id} + x_{id} \tag{2.9}$$

where c_1 and c_2 are positive constants, and $rand()$ and $Rand()$ are two random functions in the range between [0,1]; $x_i = (x_{i1}, x_{i2}, ..., x_{iD})$ represents the i^{th} particle;

$P_i = (p_{i1}, p_{i2}, ..., p_{iD})$ represents the best previous of the i^{th} particle; the symbol g represents the index of the best particle among all the particles in the population (global best); $V_i = (v_{i1}, v_{i2}, ..., v_{iD})$ represents the velocity for particle i. Equation (2.8) and equation (2.9) are the equations describing the flying trajectory of a population of particles. Equation (2.8) describes how the velocity is dynamically updated and Equation (2.9) the position update of the flying particles. Equation (2.8) consists of three parts. The first part is the momentum part. The velocity can't be changed suddenly but, it is changed from the current velocity. The second part is the cognitive part which represents private thinking of self-learning from its own flying experience. The third part is the social part which represents the collaboration among particles learning from group flying experience [15].

In Equation (2.8), if the sum of the three parts on the right side goes beyond a constant value specified by the user, then the velocity on that dimension is assigned to be $\pm V_{max}$, that is, particles' velocities on each dimension is held to a maximum velocity V_{max}, which is an important parameter, and originally is the only parameter required to be adjusted by users. Big V_{max} has particles that have the potential to fly far past a good solution area while a small V_{max} has particles that have the potential to be trapped into local minima, therefore unable to fly into better solution areas. Usually, a fixed constant value is used as the V_{max}, but a well-designed dynamically changing V_{max} might get better the PSO's performance [17].

The PSO algorithm is quite simple in concept, easy to implement, and computationally effective. The technique for implementing the PSO algorithm is as follows:

1 Initialize a swarm of particles with random positions and velocities in arbitrary dimensions D in the problem space.

2 For each particle (solution), evaluate the favorite optimization fitness function in D variables.

3 Compare particle's fitness function evaluation with its previous best p_{best} . If the current value is better than the p_{best}, then set p_{best} equal to the current value, and P_i equals to the current location x_i in D -dimensional space.

4 Detect the particle in the neighborhood with the best success so far, and assign its index to the variable g .

5 Adjust the velocity and position of the particle according to Equations (2.8) and (2.9).

6 Loop to step 2 until a criterion is satisfied, mostly a sufficiently good fitness or a maximum number of iterations.

Unlike the other evolutionary algorithms, in PSO, each particle flies through the solution space, can remember its previous best position, survives from generation to generation [17]. Additionally, compared with the other evolutionary algorithms, e.g., evolutionary programming, the original version of PSO is faster in initial convergence while slower fine-tuning [14].

2.6 Sliding Mode Control

The sliding mode control is a kind of nonlinear control that has been developed mainly for the control of variable structure systems. To be precise, it consists of a time-varying state-feedback discontinuous control law that switches at a high frequency from one continuous structure to another according to the present position of the state variables in the state space, the objective is to force the dynamics of the system in control to follow exactly the desired reference path.

The main advantage of a system with sliding mode control characteristics is that it has guaranteed stability and robustness against parameter uncertainties . Furthermore, being a control method that has a high degree of flexibility in its design choices, the sliding mode control technique is comparatively easy to implement as compared to other nonlinear control methods. Such properties make the sliding mode control greatly suitable for applications in nonlinear systems, accounting for their extensive utilization in industrial applications, e.g., electrical drivers, automotive control, etc.. [18].

For any given system, if a sliding regime occurs and the sliding manifold $\zeta = 0$ holds a stable equilibrium point P when operated in sliding mode, the feedback tracking trajectory S, regardless of its location, will be driven toward the sliding manifold, and upon reaching the manifold, it will bring the control of the system to switch on and off between two or more discrete control functions at an infinite frequency, such that the system's trajectory will be kept exactly on the sliding manifold such that $S = \zeta = 0$, and the trajectory will be directed to the desired equilibrium point P.

The whole sliding mode operation can be classified into two phases. In the first phase (named reaching phase), irrespective of the initial position of the controlled trajectory S, the SMC will force the trajectory toward the sliding manifold. This is possible through conditions, called hitting conditions which guarantee that, irrespective of the initial condition, the controlled trajectory of the system will always be directed toward the sliding manifold [19], [18].

When the trajectory touches the sliding manifold, the system enters the second phase (named sliding phase) of the control process and is also said to be in SM operation. The system will then be controlled by a series of infinite switching of its control functions such that the trajectory is kept on the sliding manifold and is simultaneously directed toward the desired equilibrium point P and finally settling at P for all future time. More importantly, by having a control process that reacts

only to the way the trajectory behaves, the trajectory will be unaffected by the effects of the parametric variations and external disturbances. In other words, the control process uses the sliding manifold as a reference path, on which the controlled trajectory will track and ultimately converge to the origin to reach a steady state without any consideration of the system's parameters and operating conditions [19].

2.6.1 Equivalent Control

The ideal sliding mode control operation is assumed to operate the system at an infinite switching frequency such that the trajectory moves precisely on the sliding manifold. However, practical limitations of devices and components in the system will alter the actual behavior of the sliding motion and induce a low-amplitude high-frequency oscillation (chattering) within the surrounding area of the sliding surface as moving toward the origin [20]. The movement of the trajectory is a consequence of the switching action $u(t)$ [21].

2.7 Electric Motors for EV Application

Electric motors are key elements in electric vehicles. The selection of traction motors for electric propulsion systems is a very important step that requires special attention and it should be carried out at the system level. From the industrial application point of view, the most common motors used in the hybrid electric vehicles (HEV) and pure electric vehicles (EV) are: DC motors, induction motors (IMs), permanent magnet synchronous, switched reluctance , and brushless DC motors. The automotive industry is still seeking the most appropriate electric-propulsion system for hybrid electric vehicles (HEVs) and even for EVs [22]-[23].

The major performance requirements of EVs electric propulsion, as mentioned in past works of literature [22] [2], [1], [24] are summarized as high instant power and a high power density, high torque at low speeds for starting and climbing, as well as a high power at high speed for cruising, a very wide speed range, including constant-torque and constant-power regions, a fast torque response, a high efficiency over the wide speed and torque ranges, a high efficiency for regenerative braking, high reliability and robustness for various vehicle operating conditions, controllability, and a reasonable cost. Based on these requirements let's evaluate the traction motors employed for EV application.

According to [22] DC motors have been important in electric propulsion because their torque-speed characteristics suit the traction requirement well, and their speed controls are simple. However, DC motor drives have complex construction, lower efficiency, low reliability, and high maintenance requirement, mainly due to the presence of mechanical commutator (brushes), even if interesting progress has been made with slippery contacts. [22] also says about the induction motors, squirrel cage induction motors are recognized as the most important candidates for propulsion of EVs, owning to their reliability, ruggedness, low cost, and ability to operate in intimidating environments. Drawbacks of the induction motor drives are high loss, low efficiency, low power factor, and low inverter usage factor, which is more serious for the high speed, large power motor. Even if the drawbacks of IM drives are to be considered during design steps, Permanent Magnet (PM) brushless synchronous motors have a number of advantages over IM, including (1) overall weight and volume are significantly reduced for given power output (high power density). (2) they have higher efficiency. (3) heat is efficiently dissipated to the surrounding. Still, PM brushless synchronous motors have a short constant power region due to their limited field weakening capability, resulting from the presence of PM field [24].

Several kinds of brushless synchronous motors have been used including the permanent magnet type and reluctance type synchronous motors. However, their capacity is limited by both demagnetization in an overload condition and the poor power factor [25]. Interior PM synchronous machines (IPMSMs) have emerged as the brightest candidates, which have been widely used for EV (or hybrid EV) traction. These electric motors may be designed with different rotor typologies, where a rare-earth magnet is often employed to achieve high-performance. However, the material cost of a rare-earth magnet is high and supply is controlled by a few countries owning the mineral resources. Some EVs adopt propulsion solutions without rare earth permanent magnet, which uses copper rotor IMs. However, in addition to the drawbacks of IMs mentioned above the starting current of IMs can be high which is disadvantageous for battery duration and the Vector controlled induction motors allow independent control on torque and flux, but the performances are sensitive to the motor parameter variation since the motor flux is estimated using the motor parameters [2].

The switched reluctance motor has several interesting characteristics that are suitable for electric vehicle drive. A switched reluctance motor operates by exciting the stator windings in response to a change in the magnetic circuit formed by the rotor and stator parts. The stator of a switched reluctance motor contains windings, similar to other electric motors, but the rotor is simply made of steel that is shaped

into salient poles, with no windings or magnets either. In a switched reluctance motor, both stator and rotor have salient poles, the stator winding consists of a set of coils, each wound on a pole, the rotor is only made with steel lamination stacked onto the shaft. This is the main difference with induction motors which have rotor wingdings or permanent magnets. Unlike an induction motor, there are no rotor bars and consequently no torque-producing current flowing in the rotor of SRMs. Switched reluctance motors can provide an effective alternative to induction motors or permanent magnet synchronous motors in many situations where the operating conditions do not suit them. One of the main drawbacks of the SRM is its high torque ripple.
Advantages of switched reluctance motor over other electric motor being used in electric vehicle propulsion are:

- Heat tolerant capability because of no winding on the rotor side.
- The rotor does not have winding since therefore no need to keep the carbon brush and slip ring assembly.
- In the absence of a permanent magnet, such motors are available at a cheaper price.
- The direction of the motor can be reversed by changing the phase sequence.
- Very high starting torque and wider speed range since it does not require field weakening technique.
- High fault tolerance capability.
- Simple braking mechanism.

2.8 Related Works

In recent years, different classes of the control approach have been found in the literature, in the control of switched reluctance motor. The raised numbers of works conducted with the control of the switched reluctance motor have been proposed starting from linear control to nonlinear control strategies such as PI control, sliding mode control (SMC) [26], Feedback linearization [12], and an intelligent approach.

The Author [26], proposed the speed control of switched reluctance motor based on feedback linearizing and sliding mode control by including the mutual inductance effect in the model. In this paper, simulation results using sliding mode control and feedback linearizing control are compared against the conventional PI control. The

comparison shows that the sliding mode controller and feedback linearizing controller have superior performance than that of the conventional PI controller. The sliding mode control parameters were selected arbitrarily based on the intuition of switched reluctance motor operation. From the simulation result of this paper, the robustness against disturbance and parameter variations of the sliding mode controller was not achieved. In addition, the responses obtained by implementing the proposed controller exhibit a speed ripple which is not practical.

The performance of the switched reluctance motor drives for electric vehicles was proposed in [27]. From the simulation results, the switched reluctance motor possesses a good dynamic response and has the fault-tolerant capability. Fortunately, this paper lacks the methodology used for designing a controller structure and it was only focused on the fault-tolerant capability of the motor.

In the paper [28], the sliding mode controller is designed and optimized using a particle swarm algorithm however, it focused on an electro-hydraulic actuator (EHA) system.

The paper in [29] proposed robust adaptive sliding mode control (RASMC) for speed control of SRM with high accuracy robust tracking performance under disturbances and parameters variation. The proposed structure can reject any external applied time-varying disturbances. The effectiveness of the proposed controller has been demonstrated by simulation and through the experiment. The simulation results verify that the proposed technique has better performance than the conventional adaptive sliding mode controller (CASMC) approach. In this paper, the adaptation parameters were selected arbitrarily and it will raise the instability of the system. The simulation results in this paper were limited to speed tracking performance only.

In this thesis, a simple structure of sliding mode control (SMC) tuned with particle swarm optimization for SRM is proposed for EV applications. It can offer the requirements of EVs such as wide speed range, high dynamic performance, minimum torque ripple and high starting torque. The torque ripple is minimized by adjusting the firing angles of the commutation system.

Chapter 3

System Modeling and Controller Design

3.1 Introduction

This chapter covers the key approaches to design a controller along with an optimization algorithm for the switched reluctance motor drive system. Section 3.2 describes the development discrete commutation pulse generation system. Section 3.3 elaborates on the design of PI current control. The design of the sliding mode speed controller is described in section 3.4 while the PSO implementation technique and torque ripple minimization are described in section 3.5 and 3.6 respectively. Moreover, the braking mechanism of an SRM is also discussed in this chapter. The controller is tested in the simulations with MATLAB®/SIMULINK® , and the simulation results are presented in chapter five.

3.2 Commutation Pulse Generation

The commutation strategy eventually regulates the performance of the SRM. Torque-speed range, machine efficiency, and torque ripples, all depend, a little, on the commutation system. For an SRM control, commutation can be described as the conversion of the desired net motor torque into a set of desired phase currents. In this thesis, a discrete type of commutation pulse generation is developed from the rotor position information. The developed commutation system is even more flexible which results in a wider speed operating range for the SRM, permits the turn-on and dwell angles to vary.

In an SRM Commutation pulse generation is a control mechanism by switching the

power converter to appropriately energize the corresponding phase winding. The rotor position is available in the model. Thus, developing gate pulses for phase A up to phase E is possible in synchronization with the rotor position θ . The switching signal is periodic over every 45^o. The designated motor has Five phases with 10/8 poles so the rotor will move 45 mechanical degrees for one complete electrical cycle. Continuous rotor position is available then it is possible to develop the commutation system that will generate the gate pulses for the converter in synchronization with rotor position.

Angular Parameters of Switched Reluctance Motor

In SRM the angular parameters are very important for controlling purposes. The following are some angular parameters used to design a discrete type of commutation for the proper excitation of SRM phase windings.
Turn-on angle: a rotor angle at the instant when a certain phase is excited.
Turn-off angle: a rotor angle at the instant when a certain conducting phase is turned off.
Dwell angle: a period in angular form in which each phase remains energized. In other words it is the difference between the turn-off angle and turn-on angle.
Advance angle: an angle that is important for the operation of the switched reluctance motor.

For the designated motor the stroke angle $s = {}^{360^o}/_{5*8} = 9^o$ which means each phase winding of the SRM conducts for 9^o But,the actual value of the conduction angles θ_m is always larger than the stroke angle s as a result of the processes of current rise and decline in the phase winding and, hence, during the operation of the SRM motor there are periods when 2 or more phase winding are in conducting state.For the case where the $T-OFF$ and $T-ON$ angles are advanced by 5^o and 8^o respectively now the conduction angle for each phase winding will changed to 12^o. The range of *on* time for switching phase A winding will then between 40^o and 28^o.

Since usually the aim is to gain high values of electromagnetic torque, the conduction period is extended within the range of strong attraction of the rotors tooth by the electromagnet made up by a pair of stator teeth so that the switch off angle slightly precedes the aligned position. For this reason, the process of current decay in a given phase is accelerated as much as possible to avoid negative torque values. This occurs after the rotor reaches the position determined by the angle $T-OFF$ as a result of energizing this winding with reverse voltage V that supplies the phase

and thus, causing the energy return to the source. Such a capability has to be held through the commutation system of the phases for the SRM.

Phase excitation sequence

Table (3.1) Commutation sequence

Phases	**Conduction period in degrees**
Phase B	$0^o - 9^o$
Phase C	$9^o - 18^o$
Phase D	$18^o - 27^o$
Phase E	$27^o - 36^o$
Phase A	$36^o - 45^o$

Since only a single coil set is activated at any one time to generate a moving field, So the sequence of the activated phases are B, C, D, E, and A for motoring mode in the model available in MATLAB. An SRM is a doubly salient type of motor, so it requires information of rotor position to energize appropriate phase which is capable of generating a torque. Hence phase A is in fully alignment position used as a reference and phase B is the next phase to be energize to generate a motoring torque. So, the commutation pulse generation system was developed in the manner shown in the table 3.1.

3.3 Control Techniques

The analytic model of switched reluctance motor can be represented by differential equations which includes voltage equations,motion equation and electromagnetic torque equation. The equivalent circuit of the motor represents voltage balance equation of the phase which consists of R-L elements. Typically,in switched reluctance motor the effect of leakage flux and mutual inductance are negligible so,they are neglected in the developed motor model. The states for the SRM are the rotor speed 'ω' and the motor current 'i' which are to be regulated by the control action. The PI and SMC are selected for controlling the states of the plant.

3.3.1 PI Speed Control for SRM

The PI speed controller is required to compare the actual speed with the reference speed and it will generate a quantity and adjust a quantity in the output which is responsible for speed control.In feedback control of SRM, the speed error is processed through the controller to regulate the magnitude of the reference current. The higher the reference current, the higher the actual current, and hence the higher the output motor torque refer equation (2.7). Therefore, a PI controller is designed in such a way that it provides necessarily a large reference current in the presence of large speed error. However, the state equations of an SRM is a highly nonlinear, conventional method for the linearized model at one operating point is not suitable in obtaining the PI gains.Thus, in this thesis the PI gains are selected by trial and error but it is impractical.

$$I_{ref}(t) = K_p e(t) + K_i \int_0^t e(t)\, dt \tag{3.1}$$

Where K_p, K_i, and $e(t)$ are the proportional gain, integral gain, and speed error respectively. But the speed error can be defined as $e = \omega_{ref} - \omega_m$. Hence,$\omega_{ref}$ is the reference speed and ω_m is the actual motor speed. The output for the speed PI controller is the command current and it can be expressed also as;

$$I_{ref}(t) = K_p(\omega_{ref} - \omega_m) + K_i \int_0^t (\omega_{ref} - \omega_m)\, dt \tag{3.2}$$

In a closed-loop, speed controlled SRM drive the speed error is processed through a proportional plus integral (PI) controller to yield the current command, The current command is also processed through another proportional plus integral (PI) controller to obtain duty cycle for the PWM controlled voltage converter. The currents are injected into a particular winding based on their position information obtained from an encoder or position estimator.

3.3.2 Design of PI Current Control for SRM

The design of a PI current controller requires a linearized model of SRM. The linearized model of SRM is developed using an ac small signal model techniques see (B.1).

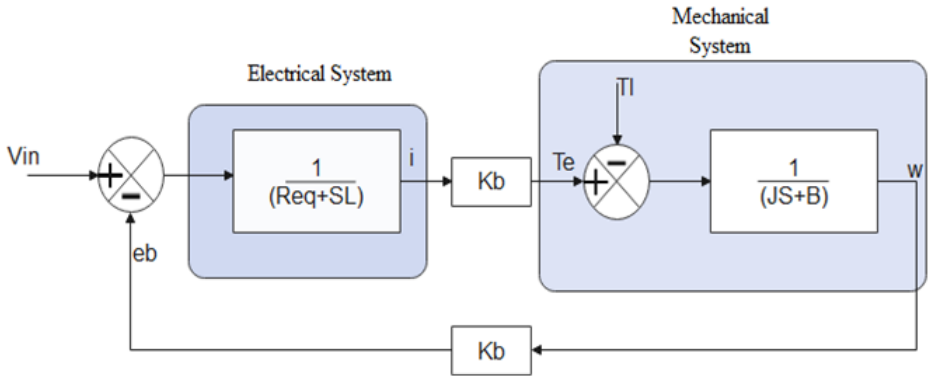

Figure (3.1) Linearized SRM model.

As shown in the figure (3.2) it is difficult to implement the current controller because,the current feedback and the back emf feedback signals are cross-coupled each other.So simplification of the above block diagram is necessary to implement a PI current controller.

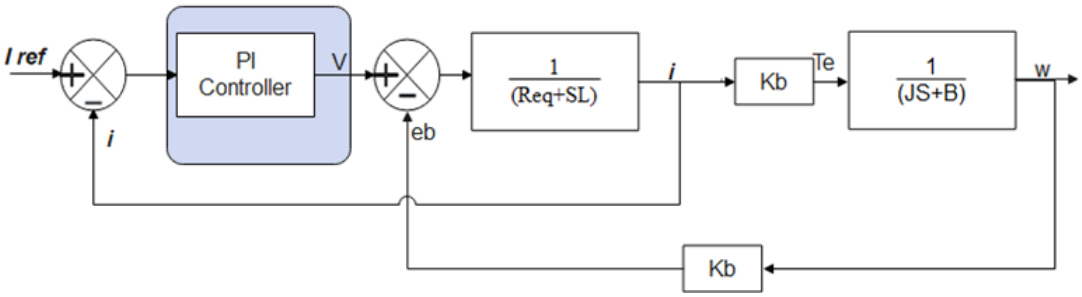

Figure (3.2) Linearized SRM model with current controller block.

$$\frac{I(s)}{V(s)} = \frac{B + js}{s^2Lj + s(LB + R_{eq}j) + R_{eq} + k_b^2} \tag{3.3}$$

Assuming a negligible electrical time constant and mechanical time constant of $T_m = j/B$ the transfer function from voltage to current become,

$$\frac{I(s)}{V(s)} = \frac{1}{LT_m}\left(\frac{(1 + sT_m)}{s^2 + s\left(\frac{1}{T_m} + \frac{R_{eq}j}{L}\right) + \frac{R_{eq}+k_b^2}{Lj}}\right) \tag{3.4}$$

To investigate the properties of the system the poles location must be known and the following substitutions are made.

$$\mathrm{b} = \frac{1}{T_m} + \frac{R_{eq}}{L} \tag{3.5}$$

$$\mathrm{c} = \frac{R_{eq} + k_b^2}{Lj} \tag{3.6}$$

Then the transfer function become,

$$\frac{I(s)}{V(s)} = \frac{(1 + sT_m)}{LT_m\,(s + T_1)\,(s + T_2)} \tag{3.7}$$

For simplicity the converter model is not included in as shown in the fig 3.3. To calculate the PI current controller gains it is necessary to find the transfer function of the inner current loop.To make the transfer function representation in standard form, the following substitution are made.

$$-T_1, -T_2 = \frac{-b \pm \sqrt{b^2 - 4c}}{2} \tag{3.8a}$$

$$G_c(s) = \frac{K_p(1 + sT)}{sT} \tag{3.8b}$$

$$T = \frac{K_p}{K_I} \tag{3.8c}$$

Where T_1 and T_2 are poles of the system,T_m is the mechanical time constant and L is the inductance which is the mean value of the aligned and unaligned inductance i.e., $L_a + L_u/2$

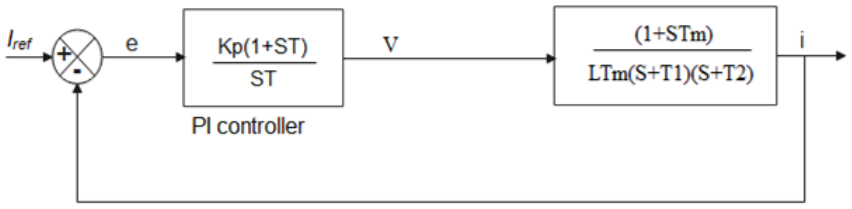

Figure (3.3) Current controller block diagram.

To design the PI current controller gains, closed loop transfer function is obtained by a simple block diagram reduction techniques as shown in the figure (3.3)

$$\frac{I(s)}{I_{ref}(s)} = \frac{K_p(1 + sT)}{LT\,(s + T_1)\,(s + T_2) + K_p(1 + sT)} \tag{3.9}$$

Now the transfer function is found in a standard form the next step is designing the PI gains i.e.,K_p and K_i. The characteristics equations for the current controller block along with the system block is a second order system, so the standard second order system is used to calculate K_p and T.

Table (3.2) Current controller design parameters

Parameter	**Value**	**Unit**
Supply voltage	400	v
Maximum current	150	A
Rated speed	1000	RPM
Rated current	20	A
Power	10	kw
Rotor friction coefficient	0.001	N.m.s
Motor inertia	0.0082	$kg.m^2$
Natural frequency	136	rad/sec
Damping coefficient	3	
Phase inductance	0.0122	H
Inductance gradient	0.018	H/rad
Phase resistance	0.3	Ω

$$T_1 + T_2 + \frac{K_p}{L} = 2\zeta w_n \tag{3.10a}$$

$$\frac{K_p}{LT} = w_n^2 \tag{3.10b}$$

To make the closed-loop step response fast without introducing too much oscillation the natural frequency w_n should be large enough. To reduce this oscillation making the closed-loop system over damped, i.e. $\zeta > 1$. Using equation (3.10) one can then have, $KP = 0.1708$ and $T = 0.007246$. The gain for integral part is $K_I = \frac{K_p}{T} = 23.57$.

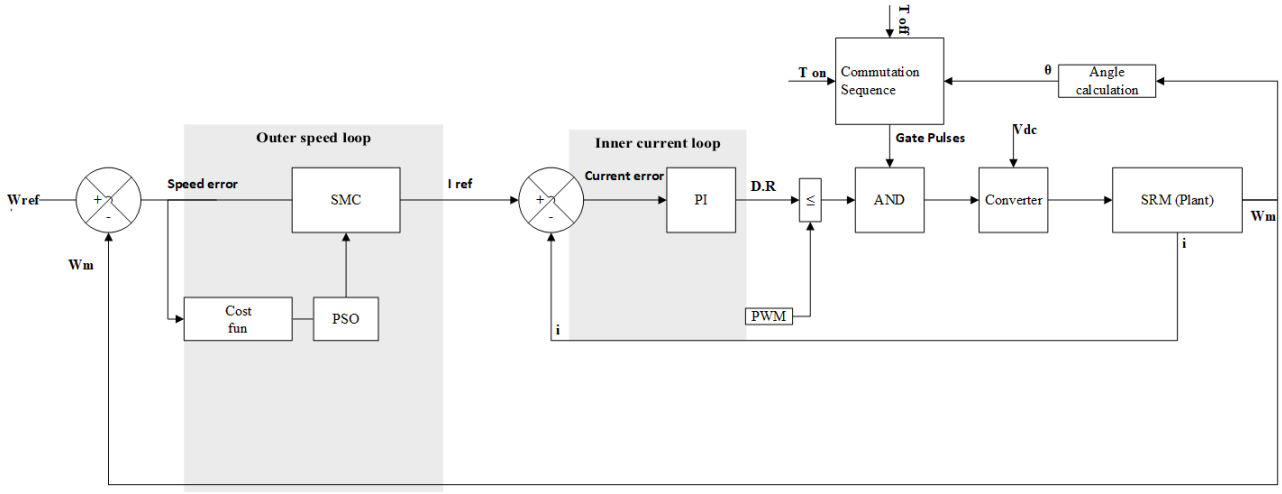

Figure (3.4) Overall system block diagram.

To illustrate how the SMC method controls the motor speed in a motor-drive system, a detailed control structure is presented in the Figure 3.4 for a better demonstration. As shown in the block diagram the control structure consists of two loops: the inner current loop and the outer speed loop. Generally, the current loop is used to obtain a duty ratio, while the speed loop guarantees that the actual speed follows the reference speed.

The torque in SRM is a function of both the current and rotor position. So current controller block is implemented along with the commutation to control the torque indirectly. As shown in figure 3.4, the outer speed loop is incorporated to generate a current reference, and an inner current loop to generate a duty ratio for a converter.

In any drive system, the rotor speed is affected by the supply voltage. The outer speed loop generates a reference current, and the current error is processed through a PI controller to generate a duty ratio. The duty ratio is compared with the constant frequency saw-toothed PWM signal having a magnitude between 0 and 1. For instance, if the duty ratio is between in the range 0 and 1 the relational operator results in a logic $'1'$, along with the commutation to force the converter switches ON. On the other hand, if the duty ratio is not in the range between 0 and 1, the relational operator results in a logic $'0'$ while a certain phase is in conduction mode. This will force the switches OFF state.

As shown in the system block diagram, the rotor position is not a part of the controller which feedbacked and compared to the reference to generate the error signal. This is appearing because the switched reluctance motor should need continuous rotor position information for the proper phase excitation.

3.4 Design of Sliding Mode Controller for SRM

The objective of the sliding mode controller is to design a sliding surface and control law that is responsible to force the system trajectories towards the sliding surface. On the sliding surface, the system is insensitive to certain parameter variations and unknown disturbances. The basic idea behind the design of any speed controller is to minimize speed error. i.e. to minimize the error to the origin of a plane formed by $e(t)$ and $\dot{e}(t)$. Graphical representation is shown in figure 3.5.

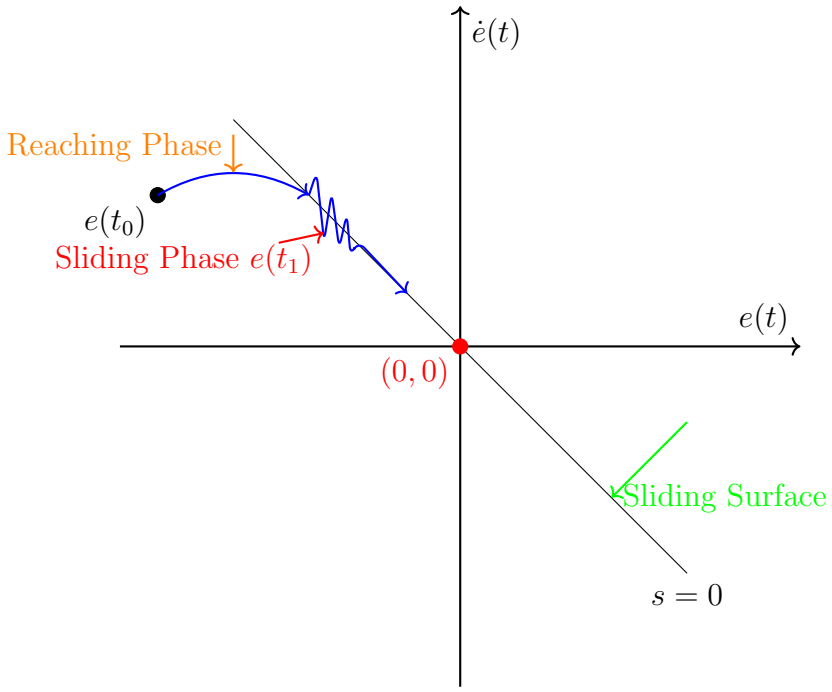

Figure (3.5) Graphical representation of sliding mode control system

The following describes the standard procedure of SMC design. We start by developing the error dynamics in a conventional form. Then, the design of a sliding manifold and control inputs are explained.

Mechanical Model

$$T_e - T_l = j * \frac{\mathrm{d}\omega}{\mathrm{d}t} + B * \omega \tag{3.11}$$

Where T_e, T_l, j, B, ω are instantaneous torque, load torque, inertia, friction coefficient, and rotor speed respectively.

Error Dynamics Development

$$e(t) = \omega_{ref} - \omega(t) \tag{3.12a}$$

$$\omega(t) = \omega_{ref} - e(t) \tag{3.12b}$$

Where $\omega, \omega_ref, e(t)$ is rotor speed, reference speed, and error respectively.

$$\dot{e}(t) = \dot{\omega}_{ref}(t) - \dot{\omega}(t) \tag{3.13}$$

And the second derivatives of the error is necessary to design a control law so,

$$\ddot{e}(t) = \ddot{\omega}_{ref}(t) - \ddot{\omega}(t) \tag{3.14}$$

Design of Sliding Surface

In this thesis, a linear type of sliding manifold is designed for the error dynamics. The error is the difference between the reference speed and the actual speed thus, bringing the sliding surface to the equilibrium point (0,0) in this case makes the error approaching zero that means the actual speed is following the reference speed regardless of parameter variation, disturbances, and initial point. This is the principle behind the sliding mode speed control of SRM and the sliding surface designed as below.

$$S = \eta e + \dot{e} \tag{3.15}$$

From the electrical and mechanical subsystems, the complete dynamic model of the SRM is expressed in the following state space form.

$$\frac{\mathrm{d}T_e}{\mathrm{d}t} = \left(\frac{\partial T_e}{\partial i}\right)(V - i_s * R - \frac{\partial \psi}{\partial \theta} * \omega)\left(\frac{\partial \psi}{\partial i}\right)^{-1} \tag{3.16}$$

$$\frac{\mathrm{d}i}{\mathrm{d}t} = (V - i_s * R - \frac{\partial \psi}{\partial \theta}\omega)\left(\frac{\partial \psi}{\partial i}\right)^{-1} \tag{3.17}$$

$$\frac{\mathrm{d}\omega}{\mathrm{d}t} = \frac{1}{j}(T_e - T_l - B\omega) \tag{3.18}$$

For speed control the second derivative of the speed become

$$\frac{\mathrm{d}\Omega}{\mathrm{d}t} = \frac{1}{j}(\frac{\mathrm{d}T_e}{\mathrm{d}t} - B\Omega - \frac{\mathrm{d}T_l}{\mathrm{d}t}) \tag{3.19}$$

Substitute equation (3.16) in to equation (3.19) one can get,

$$\frac{\mathrm{d}\Omega}{\mathrm{d}t} = \frac{1}{j}\left(\frac{\partial T_e}{\partial i}\left(\frac{\partial \psi}{\partial i}\right)^{-1}\left[V - iR_s - \frac{\partial \psi}{\partial \theta}\omega\right] - B\Omega - \frac{\mathrm{d}T_l}{\mathrm{d}t}\right) \tag{3.20}$$

For simple notation the following substitution are made

$$\beta = \frac{1}{j}\left(\frac{\partial T_e}{\partial i}\left(\frac{\partial \psi}{\partial i}\right)^{-1}\left(-\frac{\partial \psi}{\partial \theta}\omega - iR_s\right) - B\Omega - \frac{\mathrm{d}T_l}{\mathrm{d}t}\right) \tag{3.21a}$$

$$\alpha = \frac{1}{j}\left(\frac{\partial T_e}{\partial i}\left(\frac{\partial \psi}{\partial i}\right)^{-1}\right) \tag{3.21b}$$

$$\frac{\mathrm{d}\Omega}{\mathrm{d}t} = \beta + \alpha U \tag{3.22}$$

where, α and β are a function of ω, θ i, and T_l.

A Lyapunov function can be selected as, $V = \frac{1}{2}s^2$ and $\frac{\mathrm{d}V}{\mathrm{d}t} = s\dot{s}$

$$\dot{s} = \eta\dot{e} + \ddot{e} = \dot{\Omega} + \eta\Omega - \left(\eta\dot{\Omega}_{ref}(t) + \ddot{\Omega}_{ref}(t)\right) \tag{3.23}$$

Then the derivative of the lyapunov function become,

$$\frac{\mathrm{d}V}{\mathrm{d}t} = s\left(\beta + \alpha U + \eta\Omega - \left(\eta\dot{\Omega}_{ref}(t) + \ddot{\Omega}_{ref}(t)\right)\right) < 0 \tag{3.24}$$

For a constant reference speed $\dot{\Omega}_{ref}$ and $\ddot{\Omega}_{ref}$ become zero. Solving for the control signal U,

$$U = -\frac{1}{\alpha}\left(\beta + \eta\Omega + \kappa_s sgn(s)\right) \tag{3.25}$$

Substitute equation (3.25) into (3.24) gives us,

$$\dot{V} = -s\kappa_s sgn(s) < 0 \tag{3.26}$$

It is evident from equation (3.26) that, $\dot{V} = 0$ only when $s = 0$ This ensures that the the control law expressed in equation (3.25) could guarantee that $\Omega(t) \to \Omega_{ref}$ in finite time. The torque in SRM is a function of stator current and rotor position,so computing a time derivative is difficult. Thus, the torque is approximated by curve fitting method to a second order polynomial of current i. Thus,

$$T_e = 0.00145i^2 + 0.00432i \tag{3.27}$$

In this sliding mode controller design section only regulation problem is addressed i.e, constant reference speed and an alternative design method for the control input U is included in appendix (B.2)

Remark The choices of the state e in the equation 3.12b guarantees that when e converges to zero then the state ω (rotor speed) converges to its desired value ω_{ref}.

3.5 PSO Implementation to Tune the SMC Parameters

The selection of the gain for the sliding manifold and the gain for discontinuous control is usually done by trial and error or by a complex mathematical analysis which is a time-consuming task. In this thesis the cost function is selected as an integral absolute speed error (IAE), the PSO algorithm is used to tune η and k iteratively until the desired system response is achieved. The best values were obtained for $\eta = 9$ and $k = 400$ after conducting 30 iterations for 10 swarm sizes. The PSO code is developed in MATLAB which is found in the appendix (D.1)

3.6 Torque Ripple Minimization

The chief drawback of an SRM is its high amount of torque ripples, which significantly reduce the overall efficiency of the SRM drive. Torque ripple minimization is necessary for SRM drive to find an application in EV traction. The mathematical expression for the torque ripple in SRM taken from the literature [10] is as follows:

$$T_{ripple} = \frac{T_{max} - T_{min}}{T_{ave}} \tag{3.28}$$

Where,T_{max}, T_{min}, T_{ave} are the maximum possible torque, minimum torque, and averaged torque respectively.

The torque ripples in this designated motor can be minimized to a minimum possible value but it is unavoidable. Standing from the torque ripple equation, minimizing the torque ripple is done by increasing the average torque. Figure 3.6 shows the linear inductance profile and the generated torque and it is shown that each stroke generates a motoring torque in an increasing period of inductance and a generating torque in a decreasing period of inductance. Thus, by adjusting the $T-ON$ and $T-OFF$ angle of the developed commutation pulse generation along with the closed loop speed control we can minimize the torque ripples.
The converter used to supply the SRM phases is an asymmetric type of converter which consists of two switches and two diodes per phase. For example, when a certain phase is energized the two switches are turned on and in the de-energized instant both switches are turned off this mode of operation is known as 'chopping mode'. In this thesis, closed-loop PWM voltage control is used to limit the current drawn from the motor. When the load current exceeding the reference current (generated from the speed controller) the PWM comes into action by switching OFF and ON the supply, at this time current ripple occurs. From the torque equation of SRM, the torque is proportional to the square of current thus, the current ripple also affects the torque performance this has occurred in chopping mode of operation. Therefore, making the current flat-topped results in a minimum torque ripple, this is done via 'soft-switching technique' along with the phase advancement method. Soft-switching means switching a single switch at a time, which will increase the converter efficiency by reducing the power loss in the converter switch. The simulation results are available in chapter five to validate the theory stated in this section.

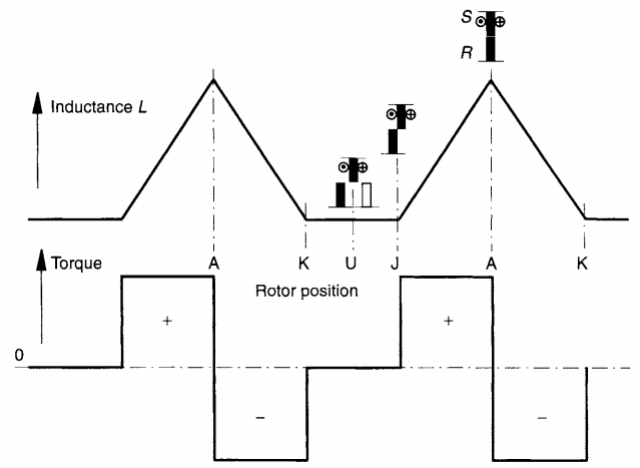

Figure (3.6) Linear inductance profile and torque of SRM [11]

Braking Mechanisms and speed reversal of SRM

The braking mechanism of the driving motor is necessary for electric vehicle traction application stopping the vehicle and charging the battery if the vehicle is a battery-powered vehicle. For regeneration operation, the converter should allow a reverse current flowing from the winding to the supply. In SRM a reverse current does not change the direction of the torque. The only way to change the direction of the torque is to excite the phase either in the increasing inductance portion (for motoring torque) or in a decreasing inductance portion (for generating torque). This would be done by adjusting the commutation. The forward motoring is done by excitation sequence B, C, D, E, and A and reverse motoring is done by the excitation sequence of E, D, C, B, and A. Then, regenerative braking is done by advancing the $T-on$ and $T-off$ angles by 36 mechanical degrees. In other words, the phase is excited in a decreasing inductance section that produces a negative (generating) torque. The name regenerative implies that when the motor is in a regenerative braking mode, there is stored energy in the phase winding flows back to the supply. Like other conventional AC machines, the reversal of speed for SRM is done by changing the sequence of phase excitation. In this case, the phase excitation sequence for speed reversal is stated above.

Chapter 4

Vehicle Design

4.1 Introduction

In this chapter, the vehicle modeling in equation-based, and torque-speed characteristics development in MATLAB/SIMULINK is conducted.
In this thesis, a 200 kg weighted vehicle is modeled in MATLAB/SIMULINK software by an equation-based approach. Some of the modeling parameters are taken from the paper [30]. The main objective of this chapter is to model the vehicle on the flat surface (no gradient resistance force), after that by developing the torque-speed characteristics of the vehicle itself and stored in a 2-D lookup table. By taking the torque of the vehicle as output from the lookup table and apply to the motor input as a load torque without any gear system (In-wheel). The torque-speed characteristic is developed arbitrarily in a linear function with time.

4.2 Motor Power Rating Calculation

Electric motors used in an electric vehicle must produce appropriate power and other characteristics i.e. high starting torque, wide speed range, high torque density, that is required for traction application. The important task is to select an appropriate rating of the motor based on the load to be carried. Vehicle dynamics is considered for selecting the proper electric motor that would provide the required power, torque, for the traction purpose. Proper selection of rating required also contributes to using an electric motor of appropriate size because the size of the motor depends on the rating. Therefore, to achieve all the traction characteristics in a compact size, a proper selection of motor rating should be done based on the load characteristics. [31],[32].

An electric motor determines the output characteristics of a vehicle in terms of power, torque, and speed. The electric motor designated for driving a vehicle must have the ability to provide sufficient power and torque to overcome the force due to load and other opposing forces acting on the vehicle body.

Table (4.1) Parameters used for vehicle modeling

Paramter	**Value**
Mass of the vehicle	$200kg$
Horizontal distance from CG to front axis	$1.4m$
Horizontal distance from CG to rear axis	$1.6m$
Height from CG to the ground	$0.5m$
Front area	$1.2m^2$
Drag co-efficient	0.4
Mass density of air	$0.4Kg/m^3$
Radius of the wheel	$0.279m$
Rolling resistance coefficient	0.02
Rated speed	$60km/hr$
Gravitational acceleration	$9.8m/s^2$
Velocity of the vehicle	$16.67m/s$
Time to accelerate to rated speed	$10sec$

Road Load, Tractive Force and Power, Transmission

According to [33], The road load consists of the gravitational force ($F_{gradient}$), rolling resistance (F_{rr}) of the tires and the aerodynamic drag force F_{ad}. The tractive force F_a provided by the main propulsion unit of the vehicle must overcome the road load ($F_{rr} + F_{gradient} + F_{ad}$) to propel the vehicle forward at the desired velocity.

$$F_{te} = F_{rr} + F_{gradient} + F_{ad} + F_a \tag{4.1}$$

Where:

$$\begin{aligned} F_{te} &- \text{Total tractive force} \\ F_{rr} &- \text{ Rolling resistance force} \\ F_{gradient} &- \text{ Gradient resistance force} \\ F_{ad} &- \text{ Aerodynamic drag force} \\ F_a &- \text{Acceleration force} \end{aligned}$$

F_{te} is the total tractive force that the output of motor must overcome, in order to move the vehicle to the desired velocity.

1. Rolling Resistance Force

Rolling resistance force is the resistance force offered to the vehicle due to the contact of tires with road. The formula for calculating force due to rolling resistance is given by the expression:

$$F_{rr} = C_{rr} * m * g = 0.02 * 200 * 9.8 = 39.2N \tag{4.2}$$

where C_{rr}, m, and g is the the rolling resistance coefficient, mass, and gravitational acceleration. But in this section,the vehicle to be modeled is on a flat road so the force contributed by the gradient force is not included here.

2. Aerodynamic Drag Force

Aerodynamic drag force is the resistant force offered due to the air acting on the vehicle body. It is largely determined by the shape of the vehicle. The formula for calculating the aerodynamic drag is given by equation:

$$F_{ad} = 0.5 * \rho * C_d * A * V^2 = 80.032N \tag{4.3}$$

where ρ, C_d, A and V is the the mass density of air, drag coefficient, frontal area of vehicle, and velocity of the vehicle.

3. Acceleration Force

Acceleration force is the force that helps the vehicle to reach a steady state speed from rest in a specified period of time. The motor torque bears a direct relationship with the acceleration force. Better the torque, lesser the time required by the vehicle to reach a given speed. The acceleration force is a function of the mass of the vehicle [32],[34].

Acceleration force can be calculated as:

$$F_a = ma \tag{4.4}$$

Assuming the vehicle reach its steady state speed in $10sec$ then,the acceleration of the vehicle can be calculated as;

$$a = \frac{V - V_o}{t_f - t_o} \tag{4.5}$$

The resulting acceleration of the car becomes $1.667m/s^2$. And the acceleration force obtained is 333.4N.

The the total tractive force in equation (4.1) be;

$$F_{te} = 39.2 + 80.032 + 333.4 = 452.632N \tag{4.6}$$

The power required to propel the vehicle in a given velocity and acceleration would be;

$$P = F_{te} * V = 452.632 * 16.67 = 7545.38watt \tag{4.7}$$

The motor selected to mount in the two wheeled vehicle has a power rating of $10kw$ so it is convenient to use this motor to propel the vehicle on a flat ground. In this thesis the main idea is to show how the motor is mounted inside the vehicle tire (In-wheeled) and to test its performance.

4.2.1 Simulation Models in MATLAB/SIMULINK environment

The equation based vehicle modeling is conducted for the calculated tractive force and vehicle parameters in table 4.1. The simulation model in MATLAB/SIMULINK is shown in the figure 4.1

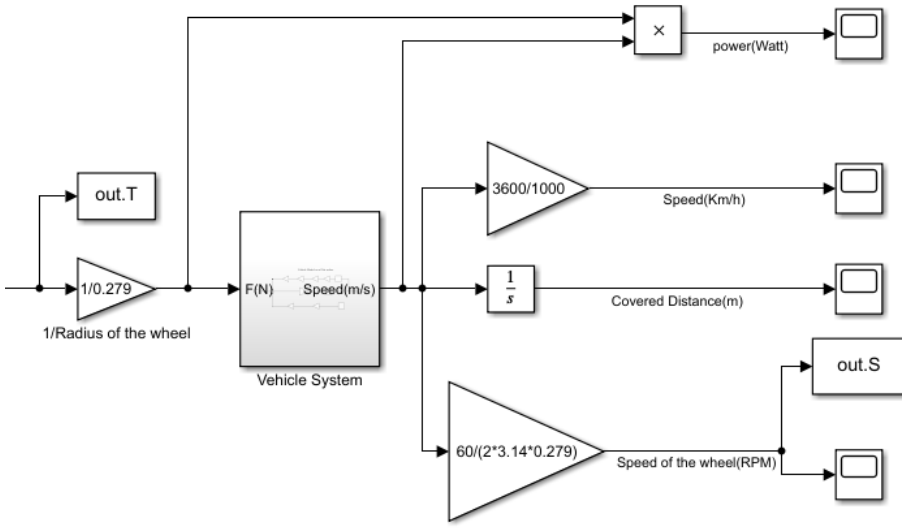

Figure (4.1) Vehicle model in SIMULINK

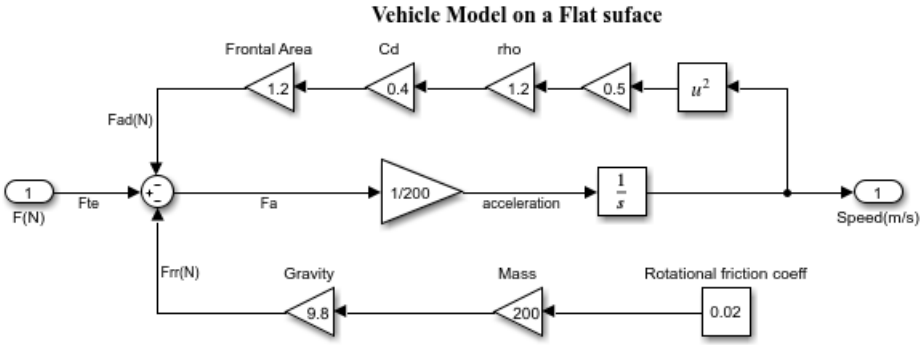

Figure (4.2) Inside vehicle system

4.3 Vehicle Characteristics

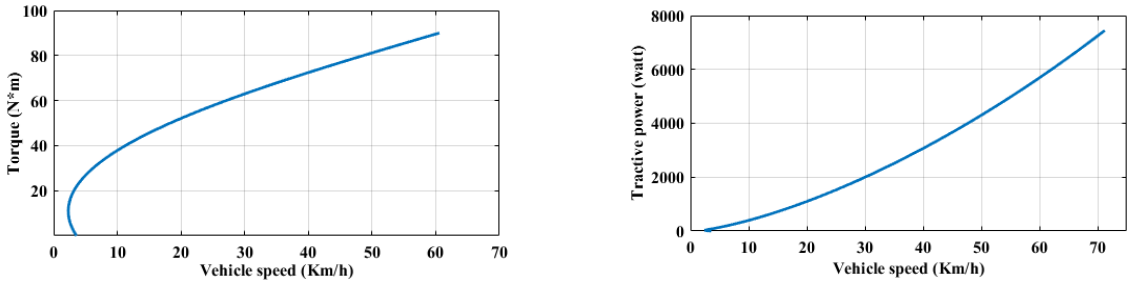

(a) Sped Vs Torque of vehicle (b) Speed Vs power of vehicle

Figure (4.3) Vehicle characteristics

Chapter 5

Simulation Results and Discussion

The simulation results are presented for a 10/8 pole SRM drive using MATLAB/SIMULINK software. The torque ripple minimization by using commutation adjustment is presented in the simulation result. The block diagram of the closed-loop drive control system, using the proposed controller, is shown in the appendix C.2. The simulation result for the SMC is presented in the second section of this chapter. The gain for the sliding surface and the discontinuous control is obtained with the help of the PSO algorithm. To show the effectiveness of the sliding mode speed controller, the performance comparison is made with the conventional PI speed controller for a constant and varying load torque. The gains for the PI speed controller are obtained by trial and error. The designated motor output characteristics are also discussed in this chapter. The performance of the SRM is tested here by loading a vehicle characteristics. To this end, the SMC parameters i.e., the sliding gain and the discontinuous control gains are obtained as $\eta = 9$ and $\kappa = 400$. Moreover, the turn-on and turn-off angles are assumed to be constant and equal to 28 degree and 40 degree respectively.

5.1 Performance of Torque ripple Minimization

The figure shown in 5.1 the motor is running without adjusting the commutation and it results that the speed is reaching around $830RPM$ in $10sec.$ figure 5.1b shows the production of excessive torque ripple in the operation of SRM which is unwanted particularly for electric vehicles where a smooth acceleration is an important feature of the performance to provide great comfort. The torque ripple also affects the speed performance. The figure 5.1a is the torque developed by the SRM and it is seen in the zoomed section, the torque is swinging between positive and negative torque regions. In this mode of operation the average torque is almost zero which means an infinite torque ripple. This is not a practical mode of operation because, it's always needed to excite the phase in advance to prevent the negative torque development

during the de-fluxing period. Figure 5.1c shows the motor current conducts for 9 mechanical degrees. Figure 5.1d represents the flux which rise up and down in each stroke. Here the simulation is made for open-loop without load torque T_l, inertia j, and friction coefficient B.

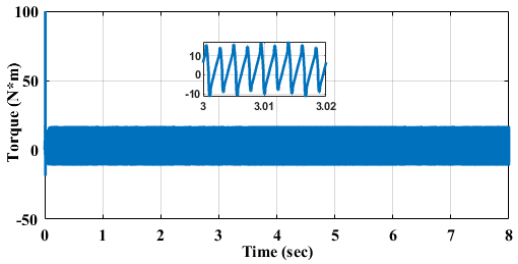

(a) Torque wave forms

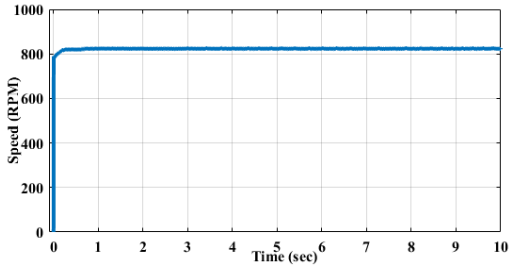

(b) Speed curve

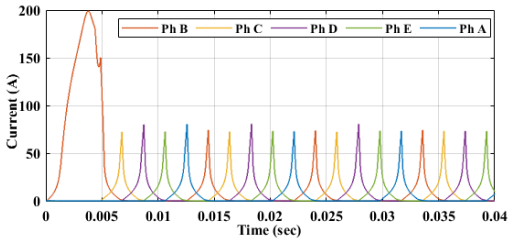

(c) Current wave forms

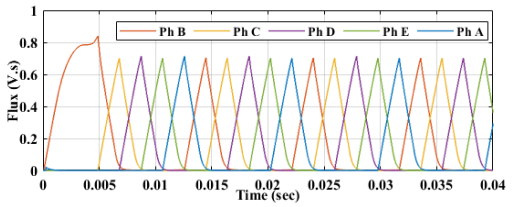

(d) Flux wave forms

Figure (5.1) Motor parameter curves without advancing $T-ON$ and $T-OFF$ angles

The figure 5.2a shows the torque developed by the SRM. Advancing the$T-ON$ and $T-OFF$ angles eliminates the generating torque and increasing the average torque. The motoring torque is only appear as shown in the zoomed section with a torque ripple of 0.85. The torque ripples here are somewhat less with advanced angles and it's also increased the average torque which is a significant issue for the SRM to be made suitable for EV applications. Fig.5.2b shows the speed of the motor which goes beyond $4500RPM$ at no-load. An increasing conduction period results in an overlap of the motor phases. This leads to an increase in the produced torque and the motor speed too. The figure 5.2c is the motor current which has a spike at starting and decreases as the speed increases this is due to the back emf development in the motor. Figure 5.2d is the flux. Here also the simulation is made for an open-loop system.

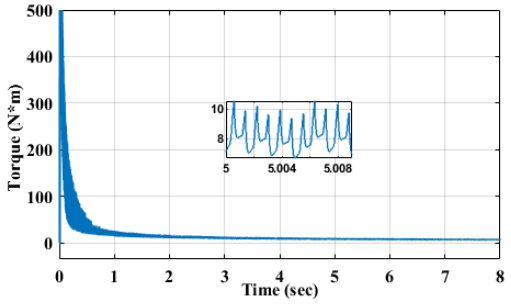

(a) Load torque wave forms

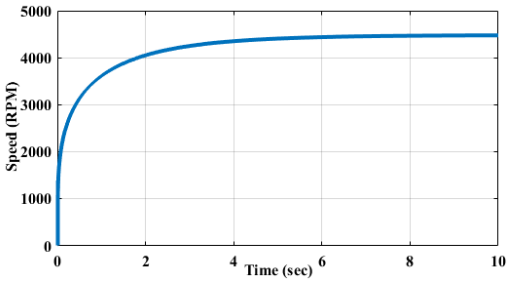

(b) Speed curve

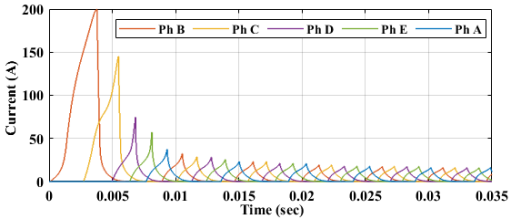

(c) Current wave forms

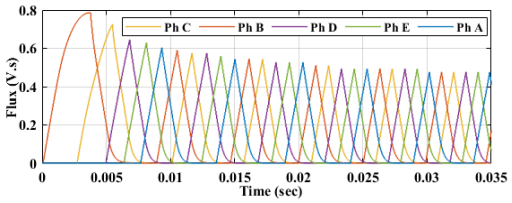

(d) Flux wave forms

Figure (5.2) Motor parameter curves with advancing the $T-ON$ and $T-OFF$ angles

5.2 Speed Tracking performance of SMC

The performance of the proposed controller structure is tested at a different desired speed while a constant load torque of $5N.m$. The figure 5.3a and 5.3b shows the speed response for a reference speed of $400RPM$ and $1000RPM$. The performance of the SMC speed controller is also tested for a staircase reference and it tracks the reference speed as shown in the figure 5.3c. The figure shown in 5.3d is the sliding surface constructed from the speed error dynamics.

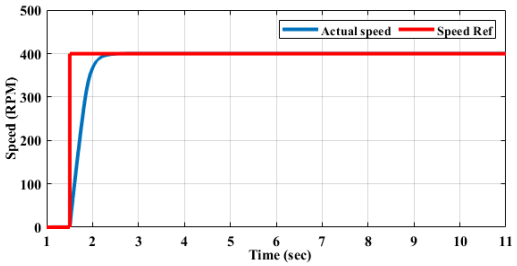

(a) Speed tracking performance for a $400RPM$ reference.

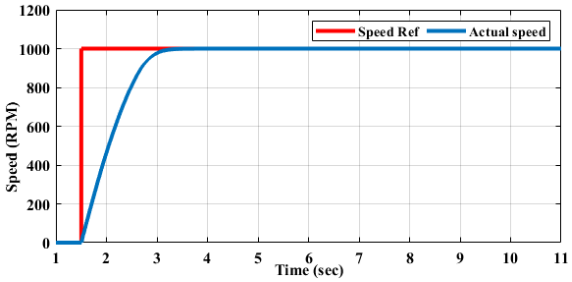

(b) Speed tracking performance for a $1000RPM$ reference.

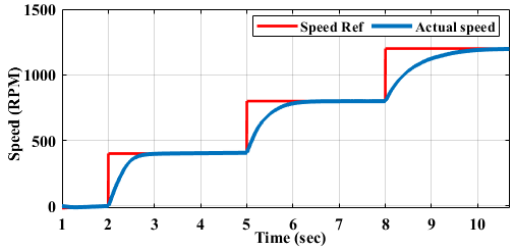

(c) Speed tracking for a stair case reference.

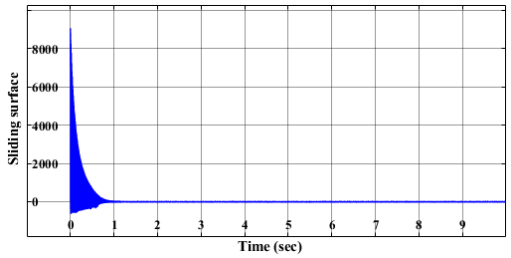

(d) Sliding manifold.

Figure (5.3) Performance of SMC at different reference speed.

5.2.1 Tracking performance comparisons of PI and SMC Under Constant Load Torque

To demonstrate the performance of the proposed controller scheme, the comparison is made with a conventional PI speed controller for the switched reluctance motor drive at a constant load torque of $T_l = 5N.m$ and while the reference speed is $1000RPM$. As the simulation result shown in the figure 5.4 the SMC has better dynamical performance than the conventional PI speed controller. The PI controller has a larger steady-state error and exhibits speed ripple compared to the SMC as shown in the zoomed section of the figure 5.4. The difference between the actual rotor speed and the reference speed for a PI speed controller is 0.18% while for the SMC is 0.0002% which validates the effectiveness of the proposed controller. For further comparison purposes, the SMC has a maximum overshoot of 0.507 and 0.975 for the PI controller.

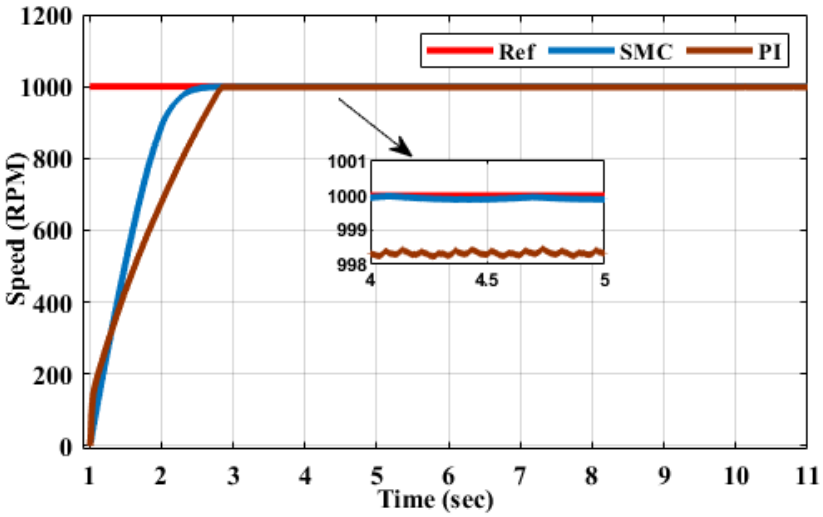

Figure (5.4) Speed Tracking performance comparison

5.2.2 Tracking performance comparisons of PI and SMC with Disturbance

The figure 5.5 gives the speed responses when the SRM is commanded to track the reference with a sudden change in load torque as a disturbance. Initially, the torque load input to the SRM is zero, and then suddenly a torque load of $10N*m$ is applied at $t = 6sec$, which results in a slight decrease in actual motor speed. Finally, the external torque load is removed at $t = 9sec.$ and then the actual speed tracks the reference speed. It is clear from Figure 5.5 that there is a deviation of actual speed using the PI controller. SMC has a small deviation to the reference speed throughout the load disturbance that makes a better choice for SRM drive. As seen in the zoomed section of the figure 5.5 the PI controller exhibits a relatively larger drop in speed response than SMC. This validates that, the SMC has better disturbance rejection capability than a conventional PI speed controller.

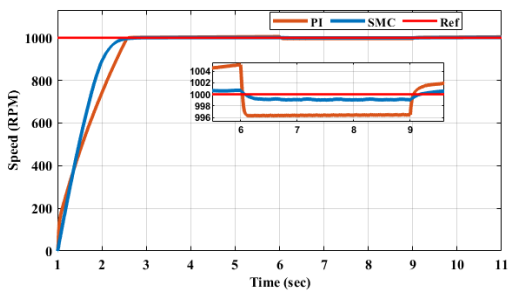

(a) Speed tracking performance comparison with disturbance.

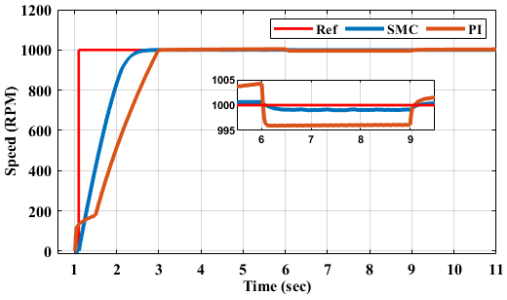

(b) Speed tracking performance for a step type reference with disturbance.

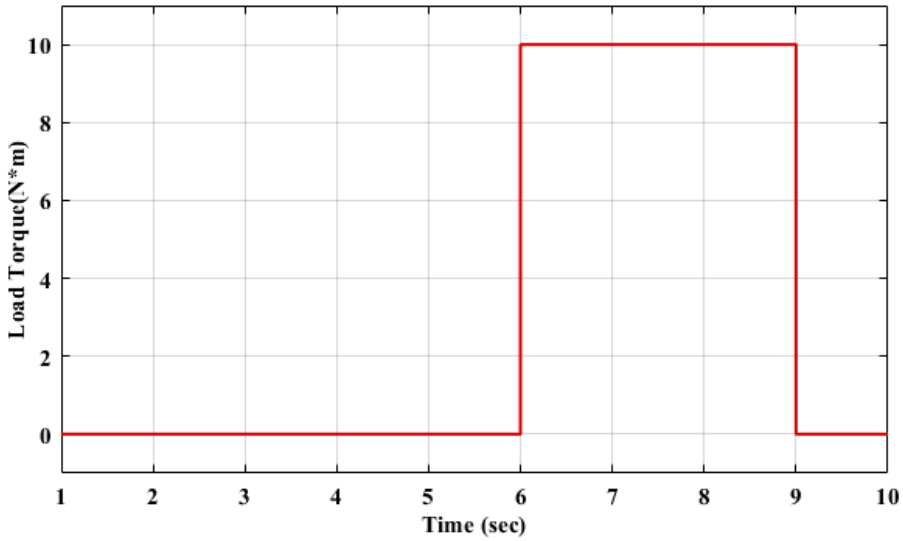

(c) Load torque as disturbance.

Figure (5.5) Performance comparison of SMC and PI speed controller with disturbance

Figure 5.5b shows the performance of the proposed controller and the PI controller for a step type reference. As shown in the zoomed section the SMC has a relatively faster response and better external disturbance rejection capability than PI.

5.2.3 Four Quadrant Operation of SRM

The SRM drive system is tested for a four-quadrant operation for a successful operation. An adjustable speed motor drive might operate in different quadrants of the speed-torque plane depending on the application. A four-quadrant operation of any machine drive is necessary to apply for an electric vehicle (EV) drive system. The figure 5.6 shows a successful operation of SRM in four-quadrant to adapt for electric vehicle propulsion.

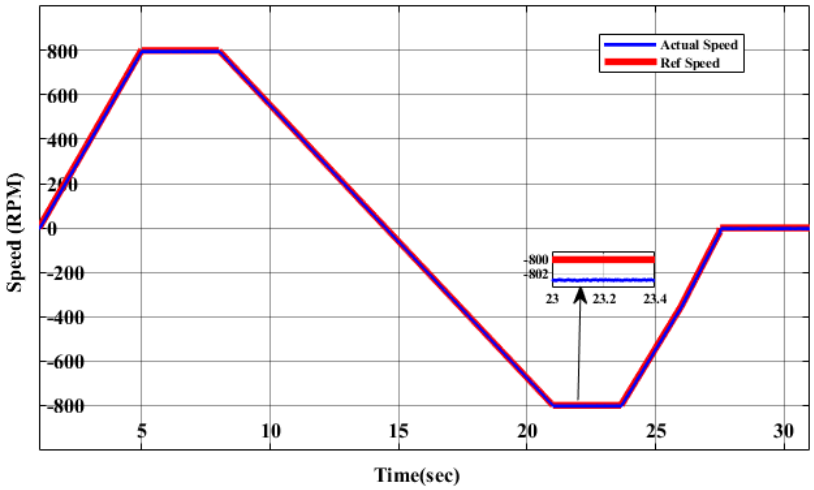

Figure (5.6) Four quadrant operation of SRM

5.3 Rotor Position Vs Motor Parameter Curves

Figure 5.7 shows the motor parameters versus rotor position θ. This is important to find out the average torque, the phase sequence, and overall motor characteristics. As seen in the figures shown below each phase conducts for 12 mechanical degrees but the actual conduction period for a single phase in the designated motor is 9 degrees. An increase in the conduction period is recommended to increase the speed of the motor. In this motor model the first phase to be excited for motoring operation is phase B as shown in the figures 5.7. The figure shown in 5.7e is the supply voltage with a varying pulse width due to PWM.

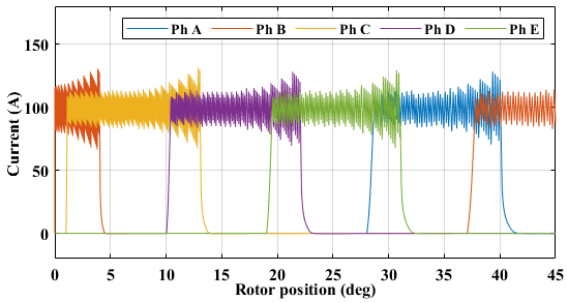

(a) Position Vs current.

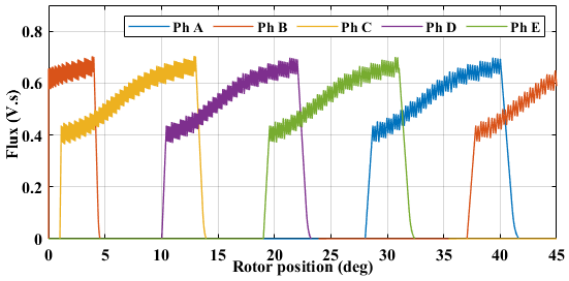

(b) Position Vs flux.

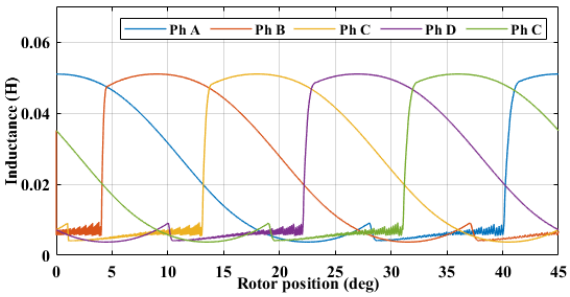

(c) Position Vs inductance.

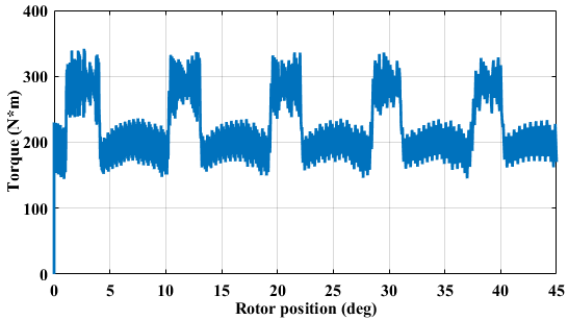

(d) Position Vs torque.

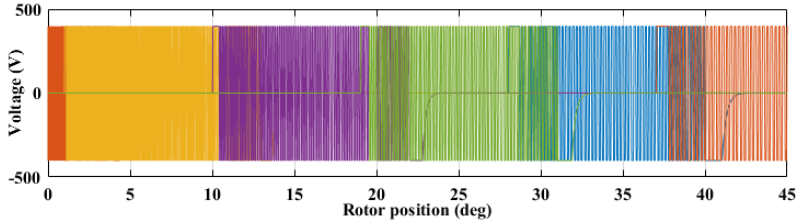

(e) Position Vs voltage.

Figure (5.7) Rotor position against motor parameters

5.4 Motor Output Curves

The following figure shows the torque and power versus speed curves of the SRM drive system. The figure in 5.8 shows motor capacity at different rotor speeds. The figure shown in 5.8a is the actual torque developed by the motor. As the figure is shown in 5.8b the power is increased linearly with speed till the base speed and it decreased at a higher speed because the torque drop is faster beyond the base speed in SRM.

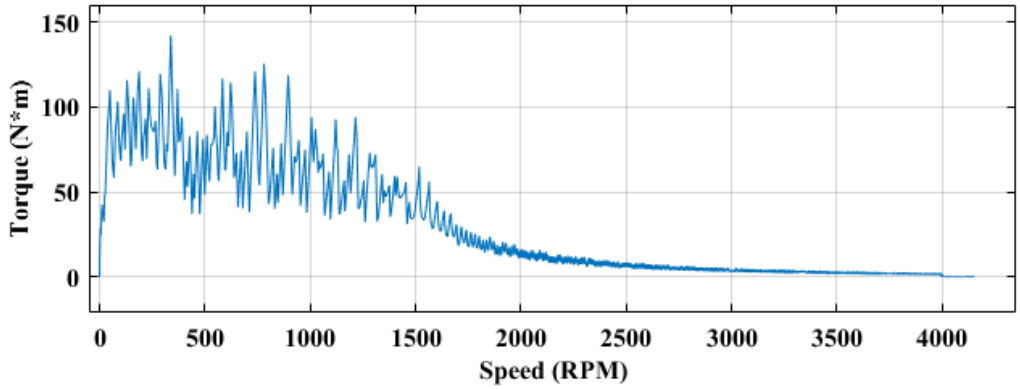

(a) Speed Vs torque.

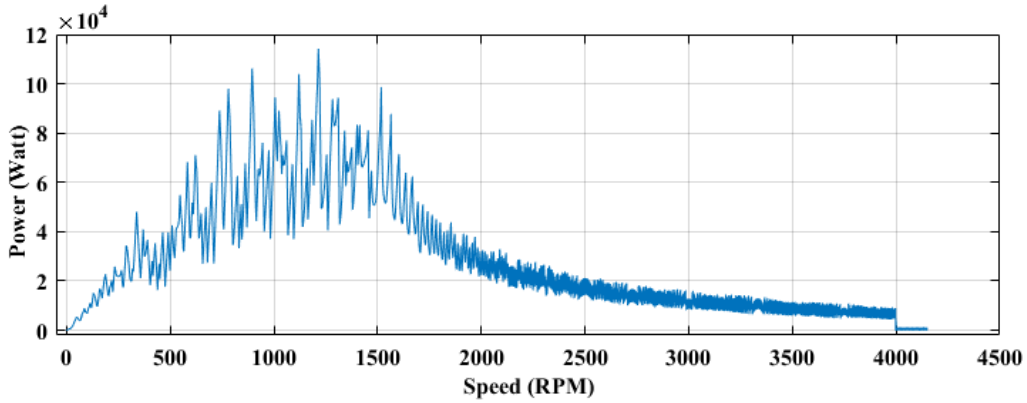

(b) Speed Vs power.

Figure (5.8) Motor output curves

5.5 In-Wheel Performance of SRM in Hard Switching Mode

The figure 5.9 shows the performance of SRM loaded with vehicle load when both the switches are **ON** and **OFF** simultaneously for each phase. Figure 5.9a is the motor speed reaches its steady-state value of $570.74RPM$ in $13sec$.The figure 5.9d shows the motor current which has a chopping caused by the PWM controlled voltage. As seen in the zoomed section there is a current chopping that directly affects the motor torque. The figure 5.9b shows the PWM controlled voltage supplied to the motor (the control signal). As seen in the zoomed section the width of the pulse is varying with a constant frequency. In this mode of operation a negative voltage $-V_{dc}$ is appearing during the recovery period this is necessary for charging battery-powered electric vehicles.

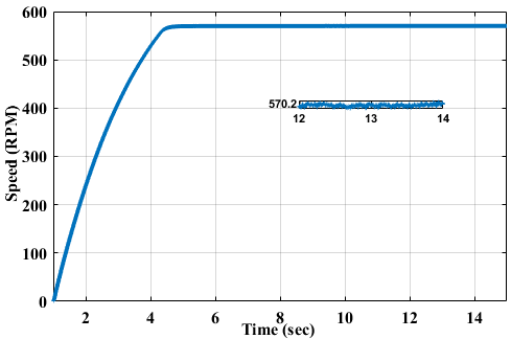

(a) Speed curve for a loaded SRM.

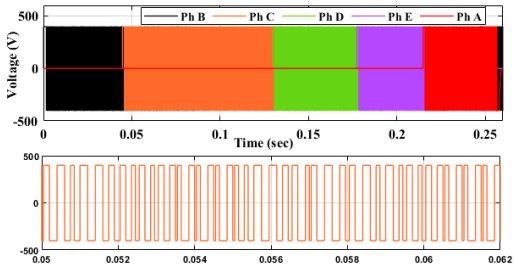

(b) Supply voltage.

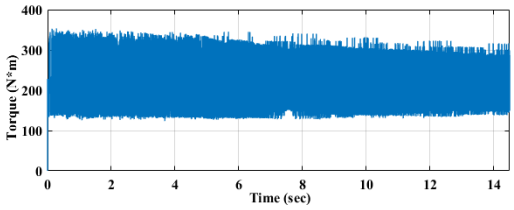

(c) Torque curve for a loaded SRM.

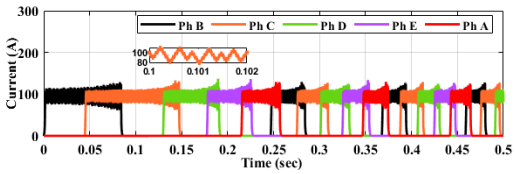

(d) Current curve for a loaded SRM.

Figure (5.9) In-wheel performance of SRM

5.6 In-Wheel Performance of SRM Using Soft Switching Technique

The soft-switching technique is also incorporated into the SRM drive. In soft-switching, both the switches are used for commutation but either the top leg or the bottom leg switch is used for control. The figure 5.10 shows the performance of SRM applying the soft-switching technique. As seen in the figure 5.10b the current has a high initial spike which results in a spike in motor torque also. In the zoomed section of the figure 5.10b the current is somewhat flat-topped this is also reflected in the torque curve.

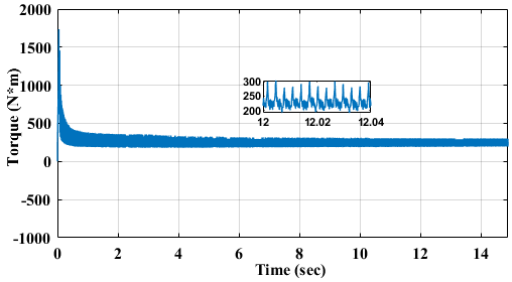

(a) Time Vs torque.

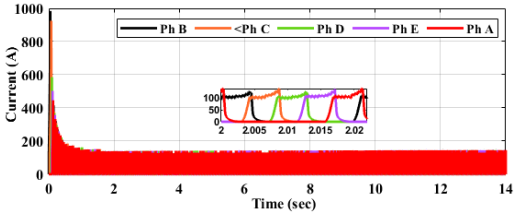

(b) Time Vs current.

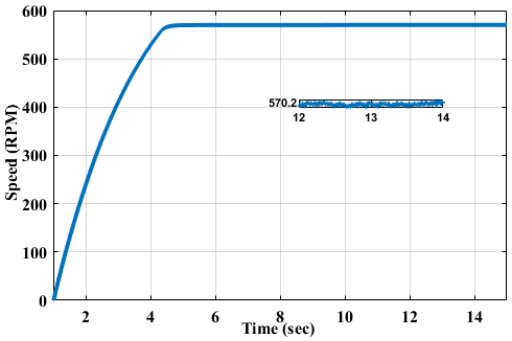

(c) Time Vs speed.

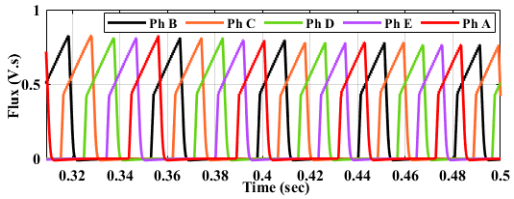

(d) Time Vs flux.

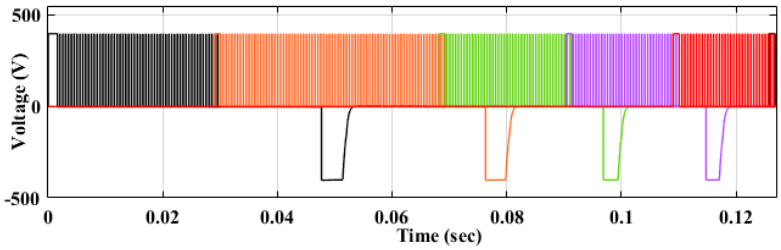

(e) Time Vs supply voltage.

Figure (5.10) In-wheel performance under soft switching technique

As seen in the figure 5.10e there is no negative voltage appearing during recovery instant. This is not suitable for regenerative braking, because during the regeneration period the power should flow from the winding to the source to charge the battery. Thus, the soft-switching technique is not suitable for electric vehicle load types.

5.7 Braking Performance of SRM

The braking operation is tested here for the loaded SRM and it shows good performance as shown in the figure 5.11a. Regenerative braking operation in SRM is different and simple from other conventional motors. As shown in figure 5.11b the torque in the regeneration operation region is negative, which makes the motor speed decreases to zero. This is done by adjusting the commutation system. The motor took 4.5*sec* to stop the vehicle while running at a steady-state speed.

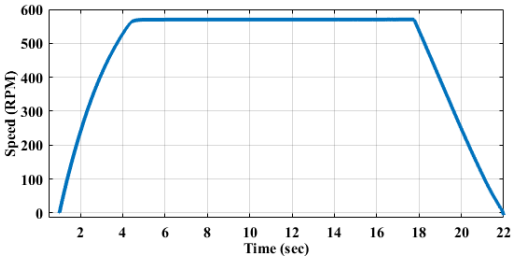

(a) Time Vs speed.

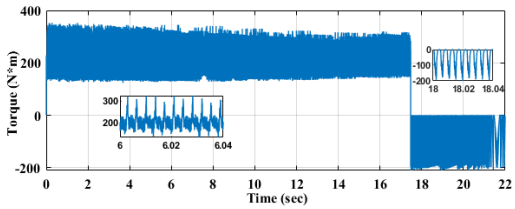

(b) Time Vs torque.

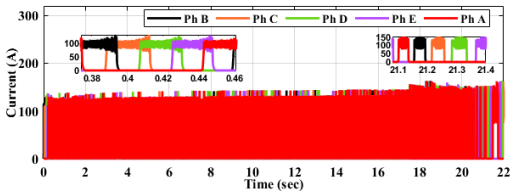

(c) Time Vs current.

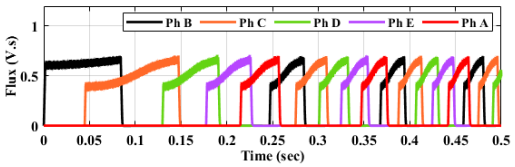

(d) Time Vs flux.

Figure (5.11) Braking performance of loaded SRM

The purpose of conducting this simulation is to show how the braking mechanism in SRM is simple and it does not include the motor torque ripple minimization during braking operation.

Chapter 6

Conclusion and Future Works

6.1 Conclusion

In this thesis, a sliding mode speed control of the switched reluctance motor with added optimality is demonstrated using simulation in MATLAB/SIMULINK environment. SIMULINK environment was used for modelling the motor and controller while a MATLAB environment was used to develop the particle swarm optimization algorithm with a cost function of an integral absolute error. The optimization algorithm was used to tune the sliding mode control parameters. Further, a commutation system is one part of the controller in SRM so, the discrete fashion of the commutation pulse generation system was developed to minimize the torque ripple.

Five phases 10/8 poles switched reluctance motor is studied in this thesis. The switched reluctance motor has a promising feature for electric vehicle traction applications. For instance, it has a high starting torque and wide speed range in which it does not require a flux weakening technique. In SRM varying the switching angles will affect the motor speed and the developed torque. Advancing the phase excitation means injecting higher current results in higher torque and higher speed. The braking mechanism of the SRM is quite simple as direction of the torque depends on the gradient of inductance with rotor position. Thus exciting the phase winding in the decreasing inductance period will generate a negative torque.

The performance of the proposed speed controller is demonstrated in the simulation result. To show the effectiveness of the proposed controller the comparison was made with the conventional proportional-integral (PI) speed controller. The speed difference between the actual and reference is 0.18 for PI and 0.0002 for SMC, which validates the SMC has a smaller steady state error than PI controller while a constant load torque of $5N.m$. The performance comparison also made for the vary-

ing load torque as a disturbance and the SMC has disturbance rejection capability while, the PI has a larger speed drop at the instant of applied load torque. Overall performance of the sliding mode controller is better than the PI controller. Thus, the sliding mode speed control is better to use as the main controller for adopting the SRM in vehicle traction applications. In addition to the speed controller, a PI current controller is incorporated as an inner loop to limit the motor drawn current depending on the speed demand.

The two-wheel vehicle is modeled in MATLAB/SIMULINK and then the torque-speed characteristic was developed that represents the vehicle load. The performance of the designated motor has been tested with a vehicle load. It took $13sec$ to reach the steady-state velocity of $60km/h$. The braking performance of the loaded SRM was also tested and it took around $4.5sec$ to stop the vehicle from its steady-state velocity.

The hard switching technique is used for the converter throughout the work but the soft switching technique was incorporated to reduce the power dissipation in the converter circuit. Lastly, the soft-switching technique is not suitable for electric vehicles, because the reverse voltage during regeneration operation is zero.

6.2 Future Works

The commutation pulse generation used in this thesis is a discrete type of commutation, which requires absolute and continuous rotor position information. Because of the discrete type of commutation the $T-ON$ and $T-OFF$ angles are set to fixed degrees for the whole application of the variable speed derive, which has an advent effect on the derive efficiency. So for future work, it is recommended that the $T-ON$ and $T-OFF$ angles can be estimated from the motor state variables i.e., speed and current depending on the speed demand.

In this thesis work, the torque ripple minimization is done for motoring operation only. But the torque ripple in the braking operation is not attempted to minimize which has an advent effect on the overall performance of the switched reluctance motor drive. For future work, we recommend minimizing the torque ripples in the generating operation region also.

References

[1] CC Chan, KT Chau, et al. *Modern electric vehicle technology*. 47. Oxford University Press on Demand, 2001.

[2] Thanh Anh Huynh and Min-Fu Hsieh. "Performance analysis of permanent magnet motors for electric vehicles (EV) traction considering driving cycles". In: *Energies* 11.6 (2018), p. 1385.

[3] Pablo Moreno-Torres et al. "Switched reluctance drives with degraded mode for electric vehicles". In: *Modeling and simulation for electric vehicle applications* (2016), pp. 97–124.

[4] Merve Yildirim, Mehmet Polat, and Hasan Kürüm. "A survey on comparison of electric motor types and drives used for electric vehicles". In: *2014 16th International Power Electronics and Motion Control Conference and Exposition*. IEEE. 2014, pp. 218–223.

[5] Nicola Bianchi et al. "Electric vehicle traction based on synchronous reluctance motors". In: *IEEE Transactions on Industry Applications* 52.6 (2016), pp. 4762–4769.

[6] XD Xue et al. "Optimal control method of motoring operation for SRM drives in electric vehicles". In: *IEEE Transactions on vehicular technology* 59.3 (2010), pp. 1191–1204.

[7] Nisha Prasad and Shailendra Jain. "Simulation of Switched Reluctance Motor for performance Analysis using MATLAB/SIMULINK Environment and use of FPGA for its control". In: *International Journal of Electrical, Electronics and Computer Engineering* 1.1 (2012), pp. 91–98.

[8] M Villani et al. "A switched-reluctance motor for aerospace application". In: *2014 International Conference on Electrical Machines (ICEM)*. IEEE. 2014, pp. 2073–2079.

[9] Jin-Woo Ahn. "Switched reluctance motor". In: *Torque control* (2011), pp. 201–252.

[10] Ramu Krishnan. *Switched reluctance motor drives: modeling, simulation, analysis, design, and applications*. CRC press, 2017.

[11] Timothy John Eastham Miller. *Electronic control of switched reluctance machines*. Elsevier, 2001.

[12] Marija Ilic et al. "Feedback linearizing control of switched reluctance motors". In: *IEEE Transactions on Automatic Control* 32.5 (1987), pp. 371–379.

[13] J Kennedy. "Particle Swarm Optimization/Kennedy J., Eberhart RC". In: *Proceeding of the IEEE International Conference on Neural Networks.–Perth: IEEE Service Center*. 1995, pp. 12–13.

[14] Yuhui Shi. "Particle swarm optimization". In: *IEEE connections* 2.1 (2004), pp. 8–13.

[15] Yuhui Shi and Russell C Eberhart. "Parameter selection in particle swarm optimization". In: *International conference on evolutionary programming*. Springer. 1998, pp. 591–600.

[16] Dongshu Wang, Dapei Tan, and Lei Liu. "Particle swarm optimization algorithm: an overview". In: *Soft Computing* 22.2 (2018), pp. 387–408.

[17] Yuhui Shi and Russell C Eberhart. "Fuzzy adaptive particle swarm optimization". In: *Proceedings of the 2001 congress on evolutionary computation (IEEE Cat. No. 01TH8546)*. Vol. 1. IEEE. 2001, pp. 101–106.

[18] Christopher Edwards and Sarah Spurgeon. *Sliding mode control: theory and applications*. Crc Press, 1998.

[19] Ahmad Taher Azar and Quanmin Zhu. *Advances and applications in sliding mode control systems*. Springer, 2015.

[20] Muhammad Rafiq et al. "A second order sliding mode control design of a switched reluctance motor using super twisting algorithm". In: *Simulation Modelling Practice and Theory* 25 (2012), pp. 106–117.

[21] Vadim Utkin, Jürgen Guldner, and Jingxin Shi. *Sliding mode control in electromechanical systems*. CRC press, 2017.

[22] Mounir Zeraoulia, Mohamed El Hachemi Benbouzid, and Demba Diallo. "Electric motor drive selection issues for HEV propulsion systems: A comparative study". In: *IEEE Transactions on Vehicular technology* 55.6 (2006), pp. 1756–1764.

[23] Nasser Hashemnia and Behzad Asaei. "Comparative study of using different electric motors in the electric vehicles". In: *2008 18th International Conference on Electrical Machines*. IEEE. 2008, pp. 1–5.

[24] Khwaja M Rahman et al. "Advantages of switched reluctance motor applications to EV and HEV: Design and control issues". In: *IEEE transactions on industry applications* 36.1 (2000), pp. 111–121.

[25] Sakutaro Nonaka and Kunio Fujii. "Brushless self-excited three-phase synchronous motor driven by voltage source inverter". In: *Electrical engineering in Japan* 103.4 (1983), pp. 81–89.

[26] M Alrifai et al. "Speed control of switched reluctance motors taking into account mutual inductances and magnetic saturation effects". In: *Energy Conversion and Management* 51.6 (2010), pp. 1287–1297.

[27] Rohit Kumar and Ravi Saxena. "Simulation and Analysis of Switched Reluctance Motor Drives for Electric Vehicle Applications using MATLAB". In: *2019 4th International Conference on Electrical, Electronics, Communication, Computer Technologies and Optimization Techniques (ICEECCOT)*. IEEE. 2019, pp. 23–28.

[28] Mohd Fuaad Rahmat et al. "Optimization of Modified Sliding Mode Control for an Electro-Hydraulic Actuator System with Mismatched Disturbance". In: *2018 5th International Conference on Electrical Engineering, Computer Science and Informatics (EECSI)*. IEEE. 2018, pp. 1–6.

[29] Mohammad Masoud Namazi, Hamid Reza Koofigar, and Jin-Woo Ahn. "Chattering-Free Robust Adaptive Sliding Mode Speed Control for Switched Reluctance Motor". In: *Control Theory in Engineering*. IntechOpen, 2020, p. 121.

[30] Jignesh A Makwana, Pramod Agarwal, and SP Srivastava. "Novel simulation approach to analyses the performance of in-wheel SRM for an electrical vehicle". In: *2011 International Conference on Energy, Automation and Signal*. IEEE. 2011, pp. 1–5.

[31] T Porselvi et al. "Selection of power rating of an electric motor for electric vehicles". In: *International Journal of Engineering Science and Computing IJESC* 7.4 (2017).

[32] Saurabh Chauhan. "Motor torque calculations for electric vehicle". In: *International journal of scientific & technology research* 4.8 (2015), pp. 126–127.

[33] Iqbal Husain and Mohammad S Islam. "Design, modeling and simulation of an electric vehicle system". In: *SAE transactions* (1999), pp. 2168–2176.

[34] Xiaodong Sun et al. "Analysis and design optimization of a permanent magnet synchronous motor for a campus patrol electric vehicle". In: *IEEE Transactions on Vehicular Technology* 68.11 (2019), pp. 10535–10544.

Appendices

Appendix A

Principles of Torque Generation in SRM

As the power is rate of change of energy,W_f ,W_m are the field energy and mechanical energy respectively.But the mechanical power is the product of mechanical speed and the developed net torque by the motor,

$$\frac{\mathrm{dW_m}}{\mathrm{d}t} = T * \omega_m = T * \frac{\mathrm{d}\theta}{\mathrm{d}t} \tag{A.1}$$

Thus,

$$i * \frac{\mathrm{d}\psi(\theta, i)}{\mathrm{d}t} = \frac{\mathrm{dW_f}}{\mathrm{d}t} + T * \frac{\mathrm{d}\theta}{\mathrm{d}t} \tag{A.2}$$

Simplifying the equation for the developed torque by the motor,

$$T(\theta, i) = i(\theta, \psi) * \frac{\mathrm{d}\psi}{\mathrm{d}\theta} - \frac{\mathrm{dW_f}(\theta, \psi)}{\mathrm{d}\theta} \tag{A.3}$$

Assuming the flux is constant,the developed torque of the motor can be expressed as;

$$T = -\frac{\mathrm{dW_f}}{\mathrm{d}\theta} \tag{A.4}$$

To express the torque in terms of current, let us define the energy stored in the field by integrating equation A.2 at constant speed becomes,

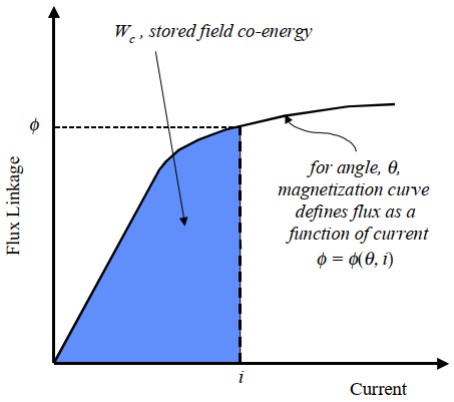

Figure (A.2) graphical interpretation of co-energy energy [9]

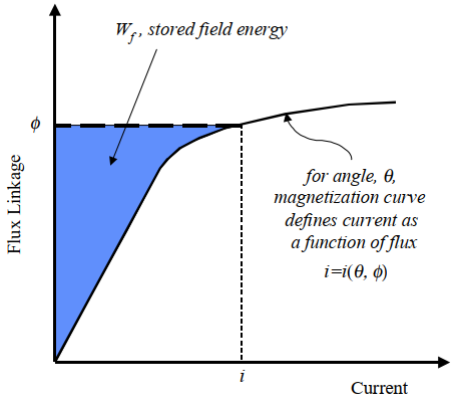

Figure (A.1) graphical interpretation of stored field energy,taken from [9]

$$W_f = \int_0^{\psi} i(\theta, \psi)\, d\psi \tag{A.5}$$

From the magnetization curve the magnetic field co-energy can be expressed as;

$$W_c = \int_0^{i} \psi(\theta, i)\, di \tag{A.6}$$

Assuming a constant current the developed torque by the motor is expressed as;

$$T = \frac{\mathrm{d}W_c}{d\theta} \tag{A.7}$$

By neglecting the magnetic saturation, flux can be expressed as-

$$\psi = L(\theta) * i \tag{A.8}$$

Where $L(\theta)$ is the motor inductance which is a function of rotor angle.

$$W_c = \int_0^i \psi(\theta, i)\, di = \int_0^i L(\theta) * i\, di = W_c = \frac{i^2}{2} L(\theta) \tag{A.9}$$

Inserting the expression for co-energy in to the torque equation gives as;

$$T = \frac{\mathrm{d}W_c}{d\theta}, but W_c = \frac{i^2}{2} L(\theta) \tag{A.10}$$

Then the simplified expression for the developed torque by the motor is as follows.

$$T = \frac{i^2}{2} * \frac{\mathrm{d}L}{d\theta} \tag{A.11}$$

Appendix B

Controller Design Section

B.1 Linearization of SRM using Small Signal Model

$$V = iR_s + \frac{\mathrm{d[L}(\theta, i)i]}{\mathrm{d}t} = iR_s + i\frac{\mathrm{dL}(\theta, \mathrm{i})}{\mathrm{d}t} + L(\theta, i)\frac{\mathrm{di}}{\mathrm{d}t} \tag{B.1}$$

But ${}^{\mathrm{d}\theta}/_{\mathrm{d}t} = \omega$, then $\mathrm{dt} = \dfrac{\mathrm{d}\theta}{\omega}$ and substituting in to the above equation become,

$$V = iR_s + \frac{\mathrm{d[L}(\theta, i)i]}{\mathrm{d}t} = iR_s + i\omega\frac{\mathrm{dL}(\theta, \mathrm{i})}{\mathrm{d}\theta} + L(\theta, i)\frac{\mathrm{di}}{\mathrm{d}t} \tag{B.2}$$

$$T = \frac{i^2}{2} * \frac{\mathrm{d}L}{d\theta} \tag{B.3}$$

$$\frac{i^2}{2}\frac{\mathrm{d}L}{d\theta} = j\frac{\mathrm{d}\omega}{\mathrm{d}t} + B * \omega + T_l \tag{B.4}$$

Perturbing the system around a steady-state operating point with small signals, the new system states and inputs are;

$$i = i_{st} + \delta i \tag{B.5}$$

$$\omega = \omega_{st} + \delta\omega \tag{B.6}$$

$$v = v_{st} + \delta v \tag{B.7}$$

$$T_L = T_{lst} + \delta T_l \tag{B.8}$$

$$\tag{B.9}$$

Where the extra subscript $'st'$ indicates steady-state values of the states and inputs, and the small signals are indicated by $'\delta'$ preceding the variables. Substituting the perturbed variables in the system equations, it is seen that the steady-state terms cancel and the remaining of these equations gives:

$$\frac{\mathrm{d}\delta\mathrm{i}}{\mathrm{d}t} = \frac{\delta v}{L} - \left(\frac{R_s}{L} + \frac{1}{L}\frac{\mathrm{dL}}{\mathrm{d}\theta}\omega_{st}\right)\delta i - \frac{1}{L}\frac{\mathrm{dL}}{\mathrm{d}\theta}i_{st}\delta\omega \tag{B.10}$$

$$\frac{\mathrm{d}\delta\omega}{\mathrm{d}t} = \left(\frac{1}{j}\frac{\mathrm{dL}}{\mathrm{d}\theta}i_{st}\right)\delta i - \frac{B}{j}\delta\omega - \frac{\delta T_l}{j} \tag{B.11}$$

In SRM the inductance,torque and back emf are a function of both current and rotor position making the dynamics highly nonlinear.To make a simple expression the following substitution are made.

$$K_b = \frac{\mathrm{dL}}{\mathrm{d}\theta}i_{st}$$
$$\delta e = \frac{\mathrm{dL}}{\mathrm{d}\theta}i_{st}\delta\omega$$
$$R_{eq} = R_s + \frac{\mathrm{dL}}{\mathrm{d}\theta}\omega_{st}$$

Where K_B, δe, and R_{eq} is the back emf constant, the back emf, and the equivalent resistance.Rearranging the

$$\frac{\mathrm{d}\delta\mathrm{i}}{\mathrm{d}t} = \frac{1}{L}[\delta v - R_{eq}\delta i - \delta e] \tag{B.12}$$
$$\frac{\mathrm{d}\delta\omega}{\mathrm{d}t} = \frac{1}{j}[K_b\delta i - B\delta\omega - \delta T_l] \tag{B.13}$$
$$\tag{B.14}$$

Current Controller

To calculate the current controller gain it is necessary to drive the transfer function of the current loop.

$$\frac{I(s)}{V(s)} = \frac{B + js}{s^2Lj + s(LB + R_{eq}j) + R_{eq} + k_b^2} \tag{B.15}$$

Assuming a negligible electrical time constant and mechanical time constant of $T_m = j/B$ the transfer function from voltage to current become,

$$\frac{I(s)}{V(s)} = \frac{1}{LT_m}\left(\frac{(1 + sT_m)}{s^2 + S\left(\frac{1}{T_m} + \frac{R_{eq}j}{L}\right) + \frac{R_{eq}+k_b^2}{Lj}}\right) \tag{B.16}$$

To investigate the properties of the system the poles location must be known and the following substitutions are made.

$$b = \frac{1}{T_m} + \frac{R_{eq}}{L}$$
$$c = \frac{R_{eq} + k_b^2}{Lj}$$

Then the transfer function become,

$$\frac{I(s)}{V(s)} = \frac{(1+sT_m)}{LT_m\,(s+T_1)\,(s+T_2)} \tag{B.17}$$

$$\frac{I(s)}{I_{ref}(s)} = \frac{K_p(1+sT)}{LT\,(s+T_1)\,(s+T_2)+K_p(1+sT)} \tag{B.18}$$

$$\frac{\mathrm{d}i}{\mathrm{d}t} = (V - i_s * R - \frac{\partial\psi}{\partial\theta}\omega)\left(\frac{\partial\psi}{\partial i}^{-1}\right) \tag{B.19}$$

B.2 Sliding mode Controller Design

Electrical Model

The applied voltage to a phase is equal to the sum of the rate of change of flux and the resistive voltage drop and is given as;

$$V = i * R_s + \frac{\mathrm{d}\psi(\theta,i)}{\mathrm{d}t} \tag{B.20}$$

Where R_s is per phase resistance,ψ is per phase flux linkage and i is the phase current.

Mechanical Model

$$T_e - T_l = j * \frac{\mathrm{d}\omega}{\mathrm{d}t} + B * \omega \tag{B.21}$$

Where T_e, T_l, j, B, ω are instantaneous torque, load torque, inertia, friction coefficient, and rotor speed respectively.

Error Dynamics Development

$$e(t) = \omega_r ef - \omega(t)$$

$\omega(t) = \omega_{ref} - e$, where ω, ω_{ref}, e is rotor speed, reference speed, and error respectively. Assuming a known constant reference speed and the rate of error becomes

$$\dot{e}(t) = \dot{\omega}_{ref} - \dot{\omega}(t)$$

but $\dot{\omega}_{ref} = 0$ $\dot{e}(t) = -\dot{\omega}(t)$

$$\dot{\omega}(t) = 1/j(Te - B * \omega - T_l))$$

$$\dot{e}(t) = 1/j(-T_e + B * \omega + T_l)$$

Computing the second derivative of error dynamics is mandatory for the sliding

manifold so the second derivative of error becomes

$$\ddot{e}(t) = 1/j\left(-\dot{T}_e + B * \dot{\omega} + \dot{T}_l\right)$$

$$\ddot{e}(t) = \frac{1}{j}\left(-\dot{T}_e + B * \dot{\omega} + \dot{T}_l\right) \tag{B.22}$$

$$\frac{\mathrm{d}T_e}{\mathrm{d}t} = \left(\frac{\partial T_e}{\partial \theta}\right)\frac{\mathrm{d}\theta}{\mathrm{d}t} + \left(\frac{\partial T_e}{\partial i}\right)\frac{\mathrm{d}i}{\mathrm{d}t} \tag{B.23}$$

$$\frac{\mathrm{d}T_e}{\mathrm{d}t} = \left(\frac{\partial T_e}{\partial i}\right)(V - i_s * R - \frac{\partial \psi}{\partial \theta} * \omega)\left(\frac{\partial \psi}{\partial i}\right)^{-1} \tag{B.24}$$

$$\dot{S} = \eta\dot{e} + \ddot{e} \tag{B.25}$$

$$\frac{\mathrm{d}T_e}{\mathrm{d}t} = \left(\frac{\partial T_e}{\partial \theta}\right)\frac{\mathrm{d}\theta}{\mathrm{d}t} + \left(\frac{\partial T_e}{\partial i}\right)\frac{\mathrm{d}i}{\mathrm{d}t} \tag{B.26}$$

$$V = U_{eq} = -PT_e + Pj\omega_{ref} - Pje - QjBe + PjT_l + iR_s + \left(\frac{\partial \psi}{\partial \theta}\right)\omega_{ref} - \left(\frac{\partial \psi}{\partial \theta}\right)e \tag{B.27}$$

$$P = \eta\left(\frac{\partial \psi}{\partial i}\right)\left(\frac{\partial T_e}{\partial i}\right)^{-1}$$
$$Q = \left(\frac{\partial \psi}{\partial i}\right)\left(\frac{\partial T_e}{\partial i}\right)^{-1}$$

Then the control signal for the sliding mode could be,

$$U = U_{eq} + U_{sw} \tag{B.28}$$

By taking the discontinuous controller as signum function to reduce chattering,the the control input to the sliding mode controller is as follows.

$$U = U_{eq} + \kappa sign(s) \tag{B.29}$$

Where U_{eq}, κ, and s is the equivalent control, any constant value, and the sliding surface respectively.

Appendix C

SIMULINK Blocks

C.1 Overall SIMULINK Block

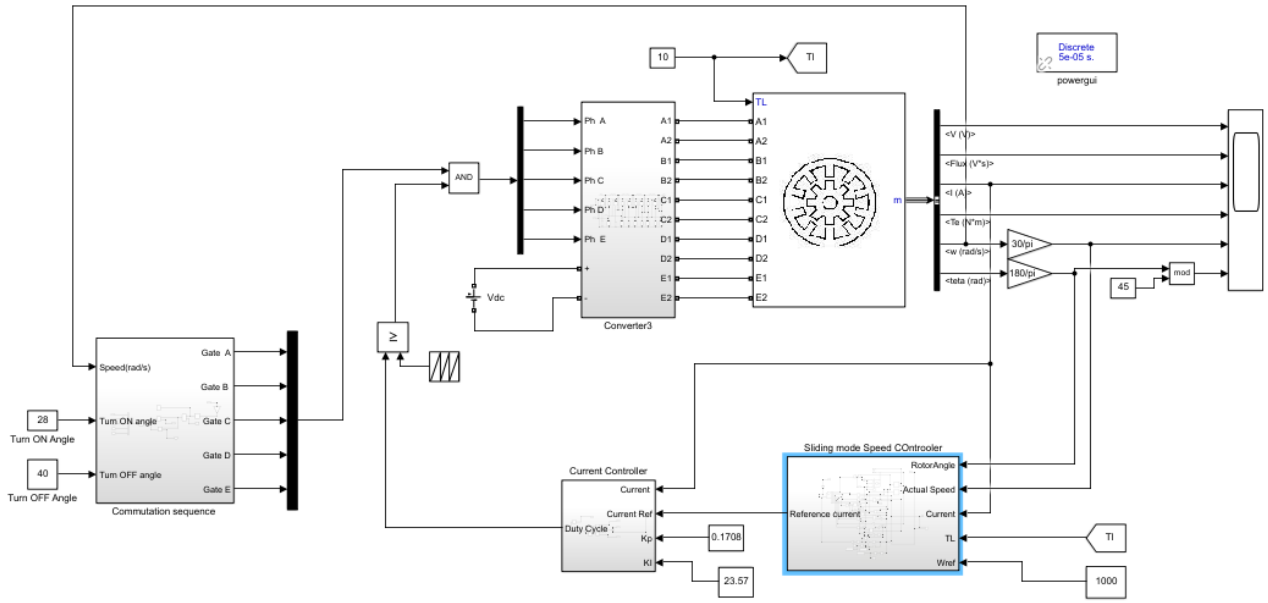

Figure (C.1) Over all simulation blocks in SIMULINK

C.2 Vehicle Loaded SRM Drive

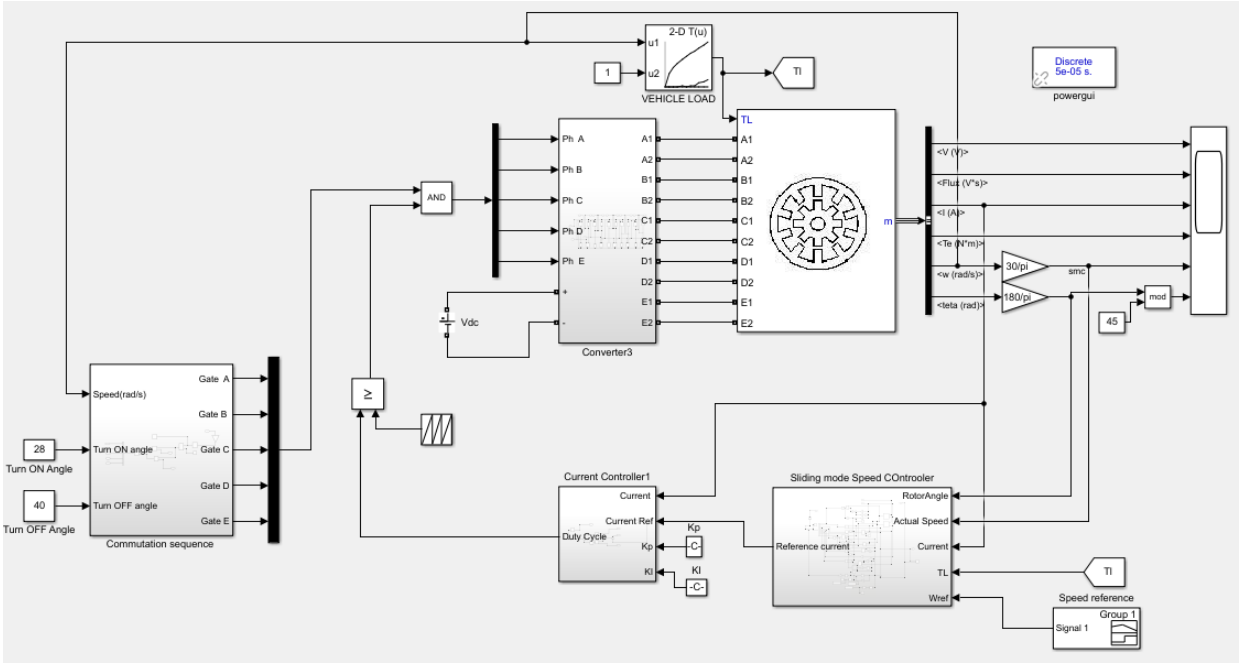

Figure (C.2) Vehicle Loaded SRM Drive

C.3 Discrete Commutation Block

The discrete commutation for a five phases 10/8 poles SRM is established in MATLAB/SIMULINK as shown in the figure C.3. To minimize the cost of the sensors the angle calculation was made from the speed sensor.When we provide a power to the SRM drive the speed of the motor is increased to a rated value and then the angle calculation block estimates the perfect position of the rotor, then the developed commutation excites the appropriate phase winding of the SRM.

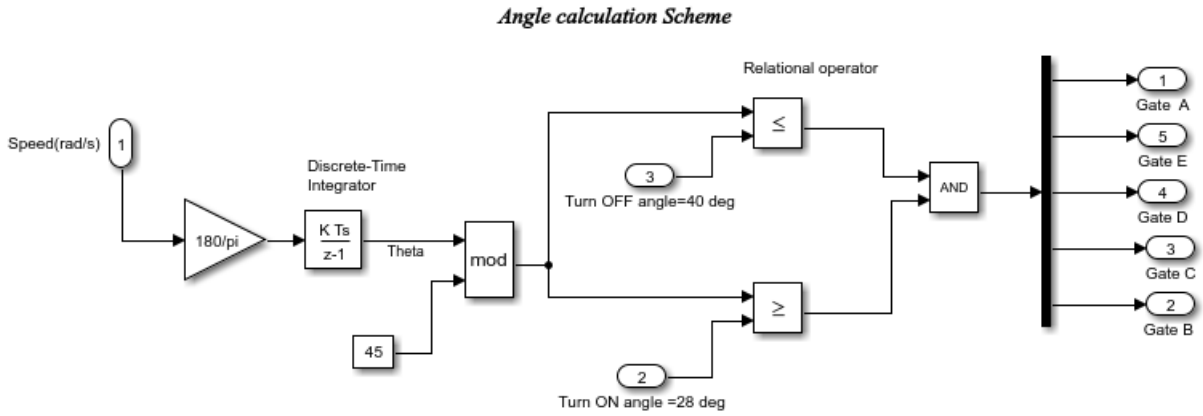

Figure (C.3) The commutation pulse generation

C.4 Ideal Power Converter

The conventional asymmetric bridge converter is used in this thesis to provide power for the motor.

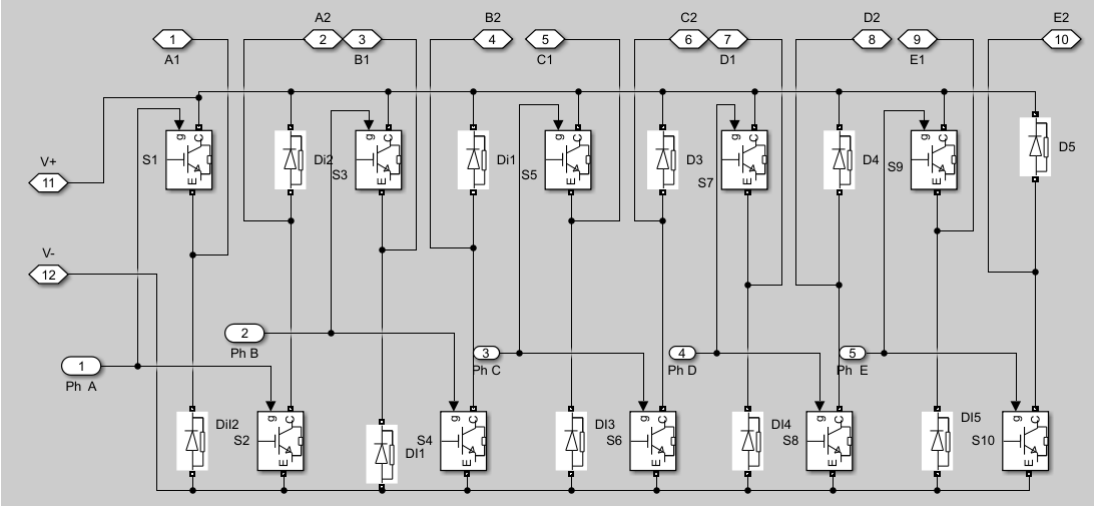

Figure (C.4) Power converter

Appendix D

MATLAB Codes

D.1 Program for Particle Swarm Optimization

```
clc                  % to clear the command window
clear                %  to clear the work space
disp('PSO_Tuned SLiding Mode Control for SRM');
%% problem setting
design_file=('slidingsp.slx');
open_system(design_file);
nvar=2;
ub=[10 450];                 % upper bound
lb=[0 350] ;                 % lower bound
obj_F=@OBJCTFUN;  % fitness function
%% algorithm parameters
Np= 10;                              % population size
maxIter=30;                          % maximum no of iteration
wMax=0.9;                            % maximum ineria weight
wMin=0.2;                            %% minimum inertia weight
c1=2;                                % acceleration cofficent
c2=2;                                % acceleration cofficent
vMax= ( ub - lb).*0.2;               %% maximum particle velocity
vMin= - vMax;                        %% minimum particle velocity

%% parameter particle population optimization

for y=1:Np
    population.particles(y).k=(ub-lb).*rand(1,nvar)+lb;
    population.particles(y).v=zeros(1,nvar);
    population.particles(y).PBEST.k=zeros(1,nvar);
    population.particles(y).PBEST.cost=inf;
    population.GBEST.k=zeros(1,nvar);
    population.GBEST.cost=inf;
end
%% main loop
for t=1: maxIter
    %% calculate the objective function
for y=1: Np
```

```
        Newk = population.particles(y).k;
          population.particles(y).cost=obj_F (Newk);
             %% update personal best value
    if  population.particles(y).cost  <  population.particles(y).PBEST.cost
            population.particles(y).PBEST. k = Newk;
            population.particles(y).PBEST.cost = population.particles(y).cost;
    end
        %% update global best value
    if  population.particles(y).cost  <  population.GBEST.cost
            population.GBEST.k = Newk;
            population.GBEST.cost = population.particles(y).cost;
    end

end
end

        %% update the K and V vectors
        w = wMax-t.*((wMax-wMin)/maxIter);
        for y=1:Np
            population.particles(y).v=w.*population.particles(y).v+c1.*rand(1,nvar)
                .*(population.particles(y).PBEST.k-population.particles(y).k)+c2.*
                rand(1,nvar).*(population.GBEST.k-population.particles(y).k);

            index1=find(population.particles(y).v>vMax);
            index2=find(population.particles(y).v<vMin);

            population.particles(y).v(index1)=vMax(index1);
            population.particles(y).v(index2)=vMin(index2);
            population.particles(y).k=population.particles(y).k+population.
                particles(y).v;

            index1=find(population.particles(y).k>ub);
            index2=find(population.particles(y).k<lb);

            population.particles(y).k(index1)=ub(index1);
            population.particles(y).k(index2)=lb(index2);
        end
        msg=['Iteration,.....',num2str(t),     'population.GBEST.cost......',
            num2str(population.GBEST.cost)];
        disp(msg);
         curve(t)=population.GBEST.cost;
        semilogy(curve(t));
grid on
  curve(t)=population.GBEST.cost;
        semilogy(curve);
        xlabel('Iteration')
        ylabel('population.GBEST.cost')
```

D.2 Program for Objective Function

```
function cost = OBJCTFUN (k)
assignin('base','k',k);
 a = sim('slidingsp','SimulationMode','normal');
    b = a.get('IAE');
    cost = b(length(b));

end
```